ORNAMENTATION AND SHELL STRUCTURE OF ACROTRETOID BRACHIOPODS

by ALWYN WILLIAMS *and* LARS E. HOLMER

ABSTRACT. The surface ornamentation of acrotretoid brachiopods includes three kinds of microstructural features which appear to reflect the nature of the periostracum and the outer mantle lobe responsible for secreting the first-formed layers of the phosphatic shell. Radial folds, less than 1 μm in wavelength, must have been casts of wrinkles in a thick, inner sealing membrane of a vesicular periostracum. Coarser folds are discrete segments of concentric ridges (fila), disposed as outwardly convex arcs (drapes) with chords up to 40 μm in length. The drapes could have been formed by spasmodic stresses within the outer mantle lobe induced by muscles controlling setae. Sporadically developed, microscopic networks of superficial grooves simulate the outlines of radially elongated vesicular cells forming the outer mantle lobe of living brachiopods, and are interpreted as casts of intercellular spaces. The grooves are continuous internally with the partitions of camerate laminae forming the secondary shell of some acrotretoids. In other acrotretoids, secondary as well as tertiary laminae contain columns and domes. The relatively smooth surfaces, bounding the laminae and defining slots within the partitions and canals within the columns, are believed to represent interfaces between organic membranes and seeded phosphatic crystallites so that the uniquely camerate and columnar nature of the acrotretoid laminae are original features of shell successions.

WITH a few notable exceptions, such as the spinose siphonotretids and the porous paterinides, inarticulate brachiopods have always been regarded as having a more modestly developed surface ornamentation than the articulates. However, this generalization only holds good for those features which can be discerned with little or no magnification. Under the electron microscope the picture is very different, the external surfaces of chitinophosphatic shells being surprisingly rich in inherent fine structures.

These microstructures are of two kinds, both frequently displayed to perfection on the surfaces of well-preserved acrotretoid shells. One group comprises sporadically occurring markings which may be categorized as epithelial imprints or as casts of strain structures developed in the bounding periostracum or in repaired areas of damaged shells. They may also arise through abnormal changes in shell secretion at the mantle edge and become manifest as growth lines. The other group consists of regular features developing periodically, or at a certain stage, or even continuously, during shell growth. They include concentric ridges (fila), superficial pits on larval shells and radial ridges (costae and costellae), respectively.

Such microstructures, which can occur on a nanometric scale, could only have been so finely preserved if the casting material had been secreted as a coat of quick-setting paste. Yet some markings also reflect the nature of the shell succession underlying this external, mineralized coat. Indeed, the extraordinary fabric of the acrotretoid shell (first described by Poulsen in 1971) is best understood when considered in conjunction with its surface expression. With that in mind, we have studied the superficial configurations and shell successions of as many genera of this micromorphic group as were available. The resultant data (Text-fig. 1) have led us to conclude that, although the ornamentation and structure of the acrotretoid shell may have been strikingly distinctive, the mantle controlling exoskeletal secretion was differentiated and functioned in much the same way as in living articulate as well as inarticulate brachiopods.

[Palaeontology, Vol. 35, Part 3, 1992, pp. 657–692, 7 pls.]

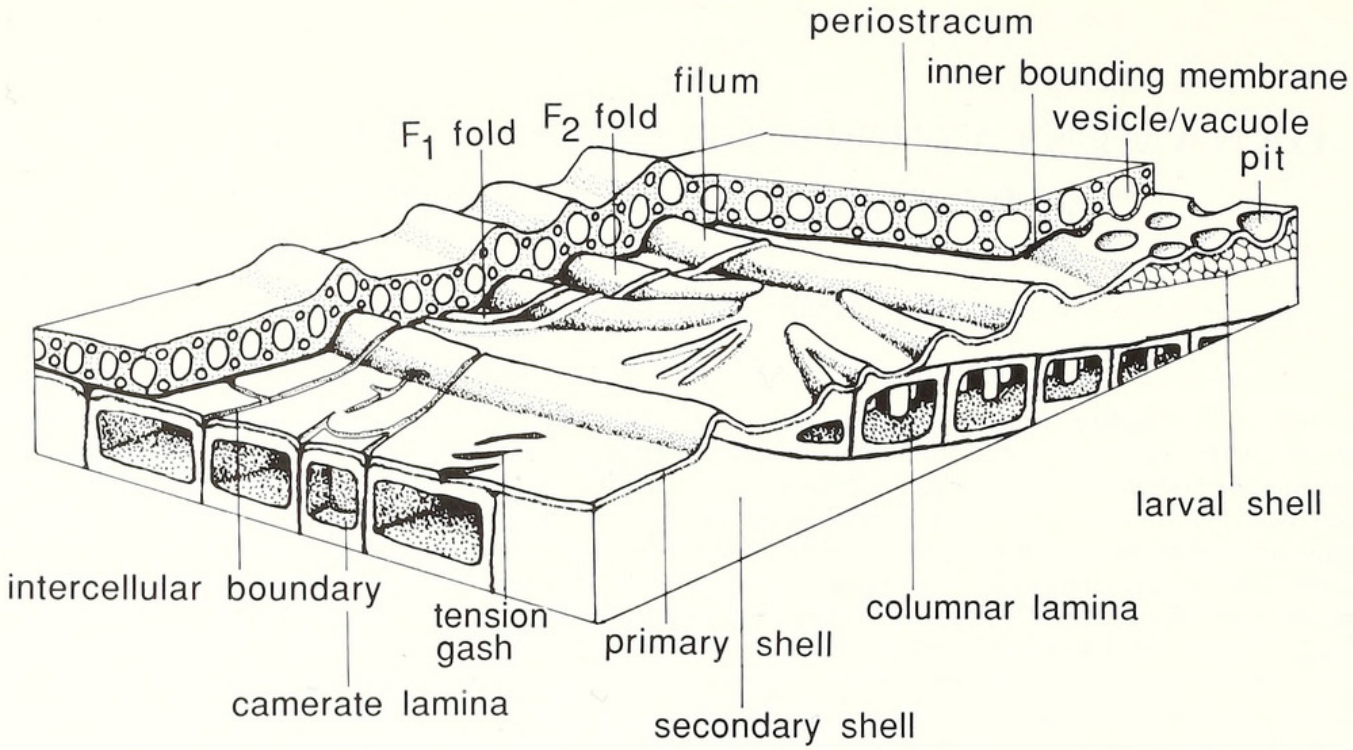

TEXT-FIG. 1. Main features of the ornamentation and shell structure of acrotretoid brachiopods relative to the inferred periostracal cover; the diagrammatic section of a camerate lamina faces anteromedially.

MATERIALS AND METHODS

The acrotretoid specimens studied for this paper were retrieved by dissolving various Cambrian and Ordovician limestones in 10 per cent acetic acid. They underwent no further preparation because of the delicacy of their shells. The surfaces of dried valves of *Glottidia* and *Lingula* were also untreated except for being freed of extraneous particles with a jet duster. The *Discina* specimens were fixed in 3 per cent glutaraldehyde and buffered to pH 7·2 with phosphate buffer, then dehydrated through an acetone series before being subjected to critical point drying.

All natural and fractured surfaces as well as polished sections were coated with gold for examination under a scanning electron microscope.

Details of specimens used to illustrate the features described in the paper are as follows:

Lingulida

Glottidia pyramidata (Stimpson), Recent, Florida.

Acrotretida

Discina striata (Schumacher), Recent, The Gambia.

Angulotreta postapicalis Palmer, Upper Cambrian Riley Formation, road south of Sandy P.O., Blanco County, central Texas (16T-6-10A(LL), Palmer 1954, p. 782).

Angulotreta triangulata Palmer, Upper Cambrian Wilberns Formation, White Creek section, Blanco County, central Texas (WC-751, Bell and Ellinwood 1962, p. 388).

Apsotreta expansa Palmer, Upper Cambrian Wilberns Formation, Threadgill Creek section straddling Mason–Gillespie County line, central Texas (TC-855-60, Bell and Ellinwood 1962, p. 388).

Conotreta? *siljanensis* Holmer, lower Viruan (Middle Ordovician) Gullhögen Formation, Gullhögen quarry, Västergötland (Holmer 1989, p. 84).

Hisingerella billingensis Holmer, lower Viruan Gullhögen Formation, Gullhögen quarry, Västergötland (Holmer 1989, p. 90).

Hisingerella tenuis Holmer, Harjuan (Upper Ordovician) Bestorp Limestone, Gullhögen quarry, Västergötland (Holmer 1986, p. 107).

Linnarssonella girtyi Walcott, Upper Cambrian Wilberns Formation, White Creek section, Blanco County, central Texas (WC-870, Bell and Ellinwood 1962, p. 388).

Prototreta sp. Middle Cambrian Meagher Limestone, Nixon Gulch, 3 Forks Quadrangle, Montano (MG 138 M4-3, Bell 1941, p. 201).

Rhinotreta muscularis Holmer, upper Viruan (Middle Ordovician), Gullhögen quarry, Västergötland (Holmer 1989, p. 115).

Scaphelasma mica Popov, upper Viruan (Middle Ordovician), Gullhögen quarry, Västergötland (Holmer 1989, p. 121).

Undescribed 'acrotretoid A', Arenig lower Latorp Limestone, Borghamn core, Östergötland, also Sjurberg section, Dalarna.

Undescribed 'acrotretoid B', Tremadoc Ceratopyge Limestone, Ottenby, Island of Öland.

Undescribed 'acrotretoid C', Tremadoc Ceratopyge Limestone, Ottenby, Island of Öland.

Specimens with number prefixed by 'L' are in the Hunterian Museum, the University of Glasgow. Those with numbers prefixed by 'Br' are in the Swedish Museum of Natural History except for 'acrotretoid A' (Pl. 2, fig. 6), which is in the Swedish Geological Survey collection (SGU) and is presently without a number.

ACROTRETOID ORNAMENTATION

The regularly developed ornament of acrotretoids consists of hemispherical or flat-bottomed pits and fila. The pits range from about 250 nm to over 5 μm in diameter and vary in distribution from hexagonal close packing to less regular arrangements with overlapping pit boundaries (Pl. 2, fig. 6). They are restricted to the external surfaces of the larval shell (Biernat and Williams, 1970) becoming faint, shallow impressions within a band no more than 10 μm wide at the boundary with the juvenile shell (Pl. 1, figs 1–2). In some acrotretoid genera, like *Rhinotreta*, the edge of the larval shell is sharply defined, usually as a raised rim, within which the boundary of the pitted ornamentation is relatively abrupt and may even intersect with the rim which bears fully developed pits. There is no significant variation in the size of the hemispherical pits distributed medianly in three dorsal larval shells of *Angulotreta postapicalis* Palmer although they tend to be smaller in the marginal zones (Pl. 1, fig. 1). In contrast, the flattened pits of *Linnarssonella girtyi* (Walcott (Pl. 1, fig. 2) and *Opsiconidion aldridgei* (Cocks) do not vary significantly in size towards the margins of their distribution.

The fila, which constitute the regular ornamentation of the post-larval shell, are equally distinctive (Pl. 1, figs 3, 5). They resemble parallel-sided anticlines with rounded crests overturned towards the valve margin where they were secreted, essentially as continuous rings or arcs of thickened shell. The rings were evidently concentric with the expanding commissure of their respective valve, but are excentrically disposed about the umbo, being most widely spaced anteromedianly. As a result, a complete filum may subtend up to four ancillary fila as anastomosing arcs in a wide-angled sector of about 240° (Pl. 1, fig. 4). In a dorsal valve of *Angulotreta postapicalis*, nine filar rings, concentrated within 55 μm of the posteromedian edge of the larval shell, are spread over 195 μm along the anteromedian vector where they subtended 15 filar arcs. The wavelength and spacing of fila increase anteriorly in *Angulotreta*: the average wavelength for 49 fila within 50 μm of the margin of the larval shell is 3·9 μm, compared with 5·0 μm for 19 fila between 250 μm and 300 μm and 8·1 μm for 10 fila between 500 μm and 550 μm anteriomedianly of the larval/juvenile shell boundary. These dimensions of the *Angulotreta* fila fall within the range noted for other genera. In the Cambrian *Prototreta* sp., for example, the fila within 50 μm and 250 μm to 300 μm of the margin of the larval shell have average wavelengths of 3·3 μm (for 14 measurements) and 4·3 μm (for 18 measurements), respectively.

Superimposed on these corrugated exteriors of the acrotretoid post-larval shell are markings of a sporadic nature. Traces of fine, impersistent, radial lineations occur rarely in *Prototreta* and about

0·03 mm² of the posteromedian surface of a ventral valve is seamed with a network of fine, shallow grooves, normally about 100 nm wide but increasing here and there to 250 nm or more (Text-fig. 2; Pl. 1, fig. 6; Pl. 2, fig. 1). The grooves delineate radially disposed, parallel-sided strips of shell, 27 of which averaged 1·5 μm wide (maximum 2·9 μm) in a 40 μm traverse. These strips are usually terminated anteriorly by wedge-shaped or lobate convergences of adjacent grooves. They are less commonly truncated by continuous transverse grooves which more frequently occur as short offsets from the radial ones. The length of the strips is accordingly variable, with the 27 measured averaging 10·8 μm and ranging from 2·0 μm to 25·5 μm.

Exfoliation of the primary shell further reveals that these grooves can be coincident with the boundaries of discrete chambers which make up the camerate secondary shell (Holmer 1989, p. 31). Valves of *Hisingerella*, for example, are frequently ornamented by a well-developed network of fine radial grooves defining parallel-sided strips, more or less identical with those of *Prototreta*, while 24 strips, in a 110 μm traverse across the interridge on a ventral valve of *H. billingensis*, average 4·6 μm (maximum 9·0 μm) in width. In places where the primary shell is missing, the grooves are seen to be continuous with narrow slits between the walls of adjacent camerae in the underlying secondary shell (Holmer 1989, fig. 26D; Text-fig. 3; Pl. 2, fig. 2). There can be little doubt that these grooves were the casts of intercellular boundaries but of a specialized type of epithelium, as will be discussed later.

Before describing the superficial fold systems, we have to identify those features which may be similar in morphological style, but which were growth adjustments to shell damage or malformation. Neither of these conditions commonly affected the acrotretoid shell, but two examples are described to illustrate the criteria used in distinguishing the fold systems under scrutiny.

The effects of shell damage and malformation are well displayed in a single dorsal valve of *Prototreta* and confirm that these phenomena are usually related. The zone of shell damage, which extends radially for about 200 μm and disrupted 10 fila, is marked by two sets of slit-like indentations (Text-fig. 4A; Pl. 2, fig. 4). We have interpreted one set as gashes in a radially disposed scar originating at a fracture in the shell; the other, an *en échelon* set, as having been formed in a lateral shear zone, parallel with the trace of tissue undergoing repair. Some of the latter tension gashes are associated with minute folds superimposed on fila, which are consistent with the assumed stress fields.

Malformations, excluded from our analysis of the acrotretroid fold systems, are sets of fila which are disposed asymmetrically about an axis (or axes) and skewed relative to radial and concentric traces on the shell. Although malformations are here distinguished from *in vivo* fractures of the shell, the majority were probably propagated in stress fields set up when such injury was inflicted. For example, the malformation shown in Text-figure 4A (see Pl. 2, fig. 3) is about 200 μm posterolaterally of the zone of damage illustrated in the same Text-figure. It involved ten fila, in a 150 μm band,

---

EXPLANATION OF PLATE 1

Fig. 1. *Angulotreta postapicalis*. L14899A; diminution and loss of hemispherical pits towards the margin of a dorsal larval shell with draped fila in the lower median sector of the micrograph, × 700.

Fig. 2. *Linarssonnella girtyi*. L14898; fading of discoidal pits towards the margin of a dorsal larval shell at the left-hand edge of the micrograph, × 3200.

Figs 3–4. *Angulotreta postapicalis*. 3, L14899B; external view of dorsal valve showing concentric fila and their interruption into sets of drapes, × 83. 4, L14899B; an enlargement of the right posterolateral sector of the dorsal valve to show the anastomosing nature of the fila, × 410.

Fig. 5. 'Acrotretroid A'. Br 133879; external view of dorsal valve showing the interruption of fila into radially disposed sets of drapes, × 78.

Fig. 6. *Prototreta* sp. L14900A; external view of posterolateral surface of a ventral valve showing a network of interconnected grooves superimposed upon fila, × 2050.

All scanning electron micrographs.

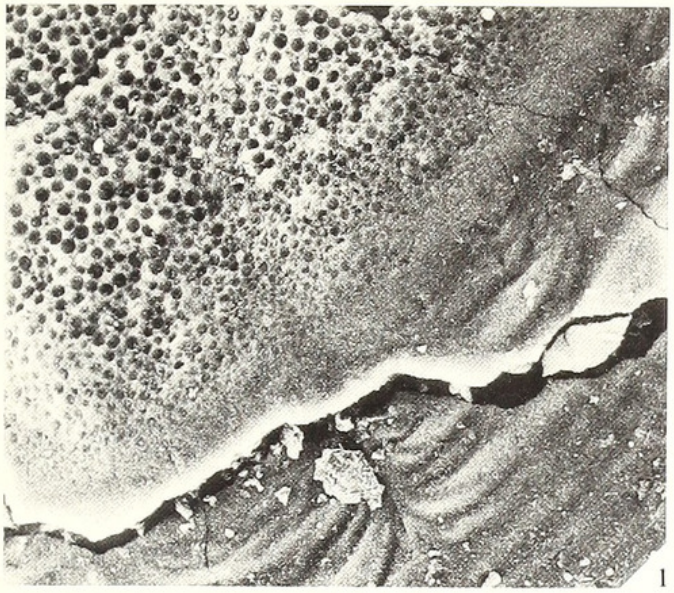

1

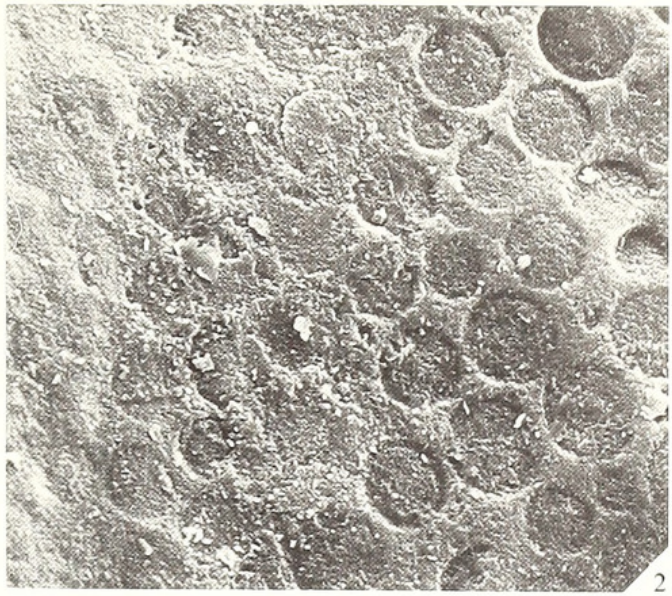

2

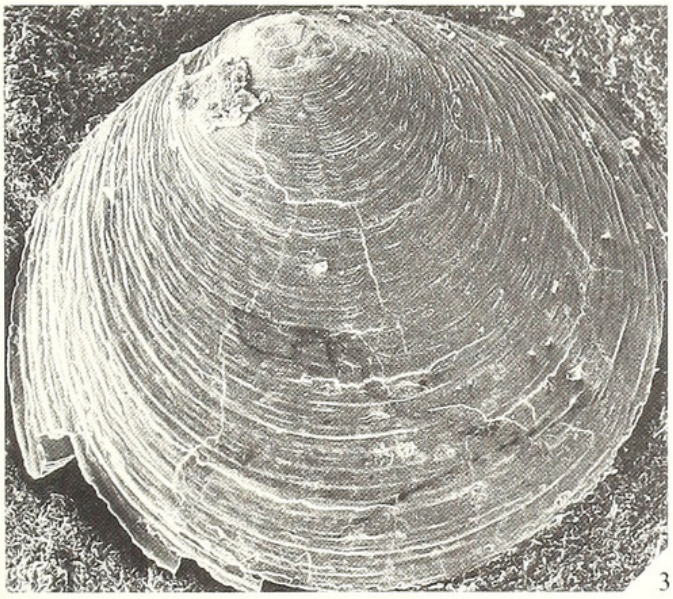

3

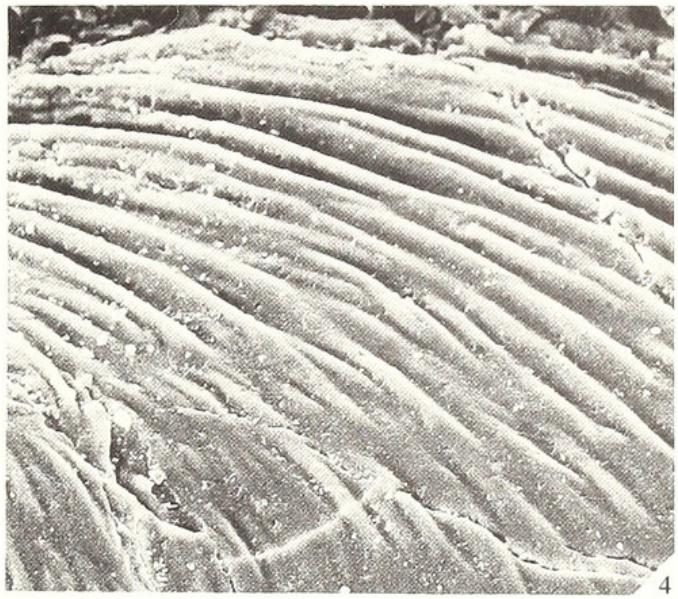

4

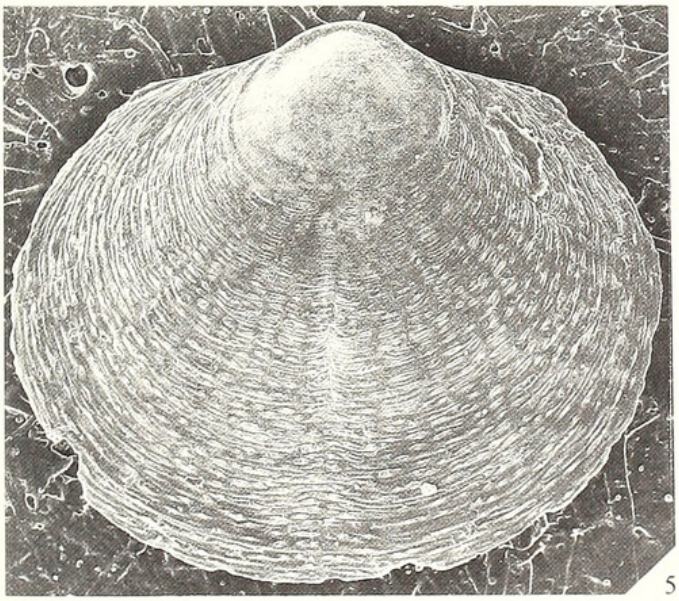

5

6

WILLIAMS and HOLMER, acrotretoid brachiopods

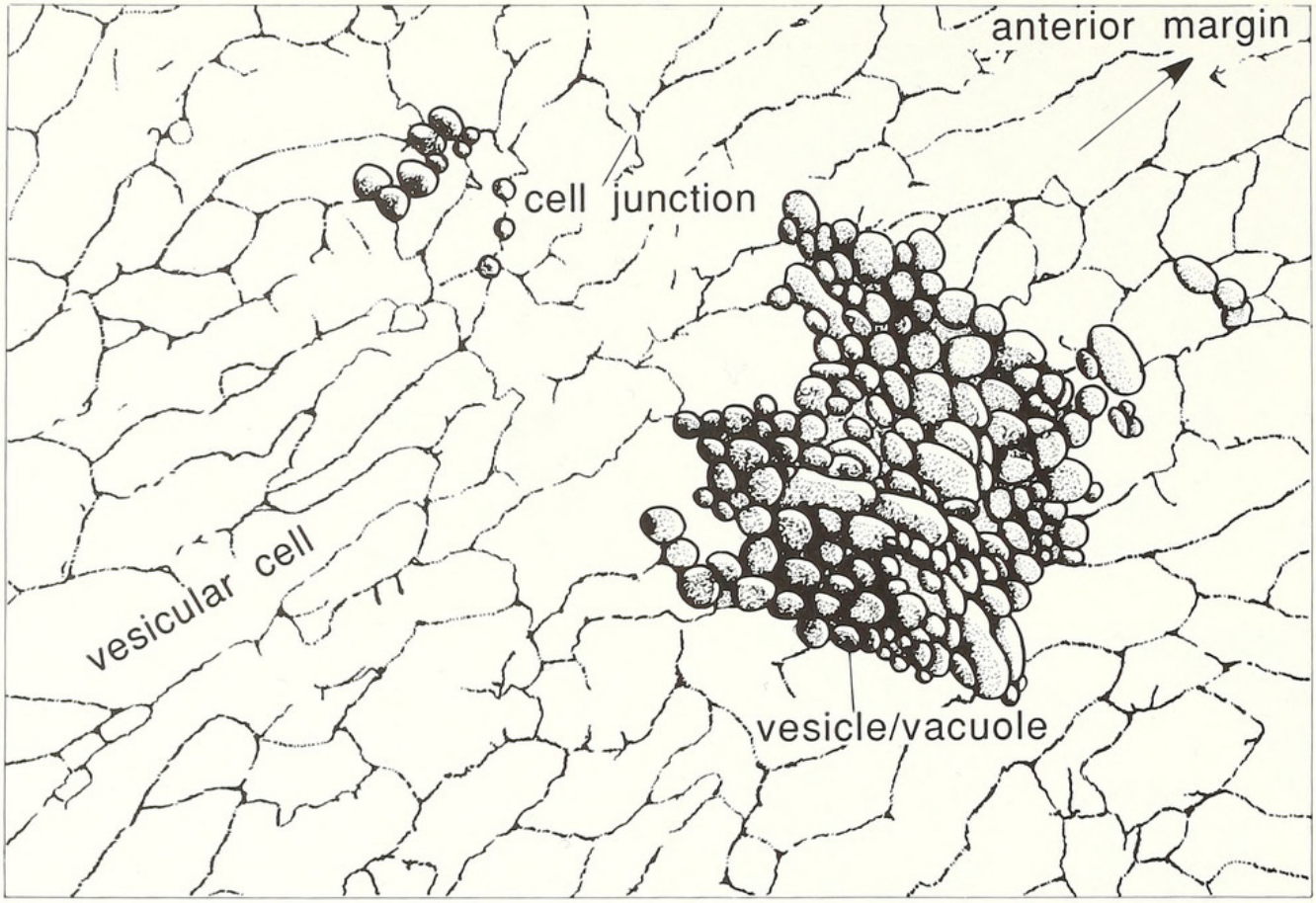

TEXT-FIG. 2. Interpretation of a tracing of markings on the posteromedian exterior of a ventral valve of *Prototreta* sp. as casts of vesicular cells (see Pl. 2, fig. 1).

which have been skewed along axes subtending an anterior angle of 30° with the valve radius. The relationship suggests that the malformed band was secreted by a strip of torn mantle edge before it became fused with the scar tissue in the damaged zone.

The fold systems, which are such distinctive components of acrotretoid ornamentation, are of two types. Both look like flexures or waves in the deformational sense and the finer sets are so in every respect. The coarser folds, however, are really segments of consecutive fila disposed as variable sets of short, adjacent arcs which are always outwardly convex like drapes of cloth hanging between short loops of cord (Text-fig. 4B; Pl. 2, fig. 5; Pl. 3, fig. 1). The basic units, the filar segments, were therefore genetically rather than mechanically induced, but they can be interpreted as flexure systems relative to the mantle edge and are conveniently so described.

Filar (F_2) folds (drapes) usually occur in arcuate sets which vary in spacing as well as in individual width and chord length. In *Angulotreta*, for example, 20 or so sets of drapes occasionally form continuous bands, up to 40 μm broad medioradially, which can be traced around a valve to its posteromedian pseudointerarea. A modal count of three drapes (range 2–7) was obtained for 72 sets developed in a concentric band, 200 μm broad medioradially, on a juvenile dorsal valve of *Angulotreta*. Each set usually starts abruptly at, or as an encroachment on, the anterior face of a filum which forms a continuous posteromedian boundary so that successive drapes tend to become more convex radially and may even overlap onto a succeeding continuous filum (Text-fig. 4B).

The first-formed drapes seldom indent the margin of the larval shell, beyond which they immediately occur. However, the antero-median edges of two out of three circular larval dorsal valves of 'acrotretoid A' are deeply notched for up to 20 μm by the nick points of two submedian sets of drapes. These nick points persisted throughout shell growth to form a deep, median trough

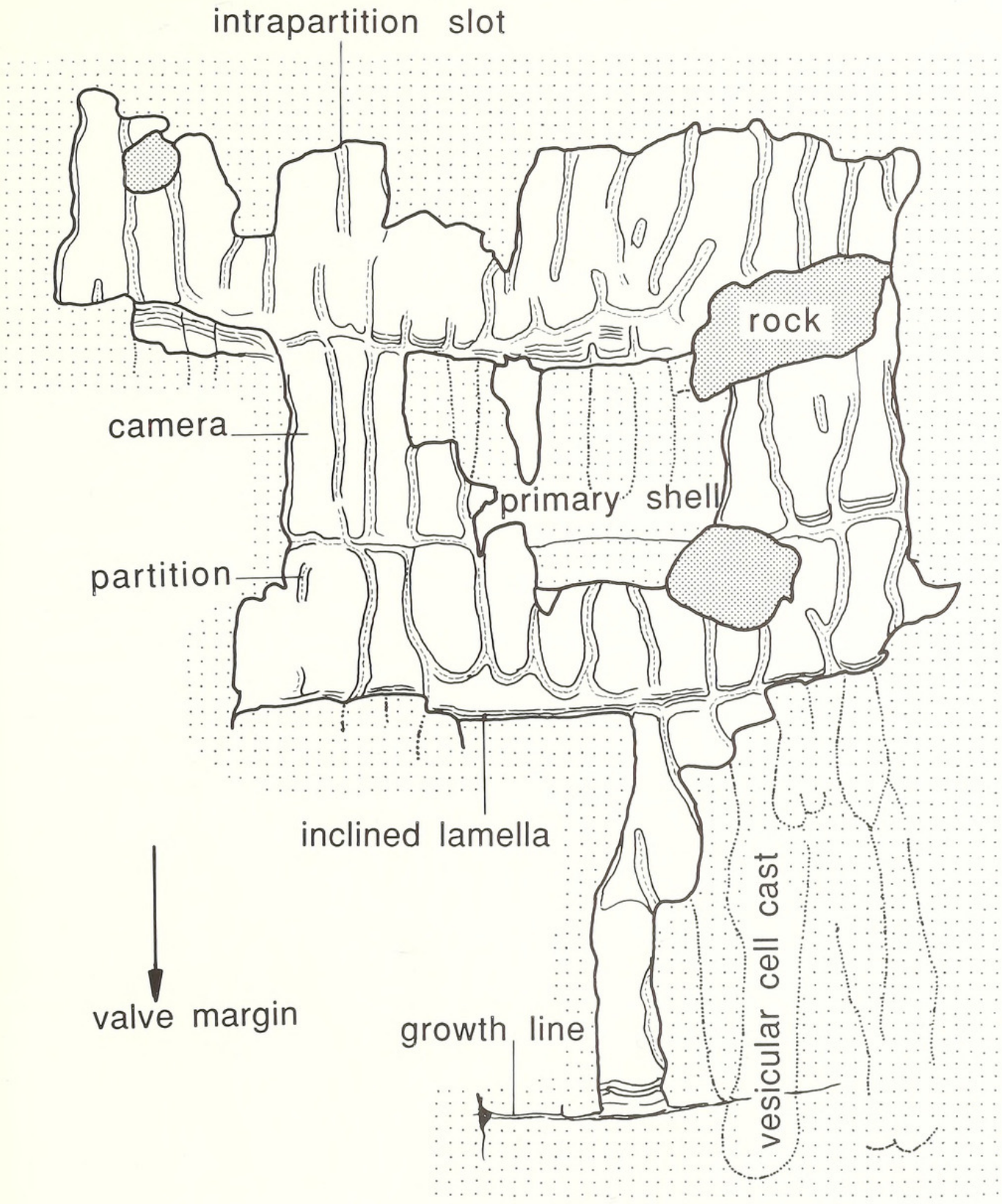

TEXT-FIG. 3. Interpretation of a tracing of grooves and ridges on the partly exfoliated exterior of a dorsal valve of *Hisingerella billingensis* as casts of vesicular cells (Pl. 2, fig. 2).

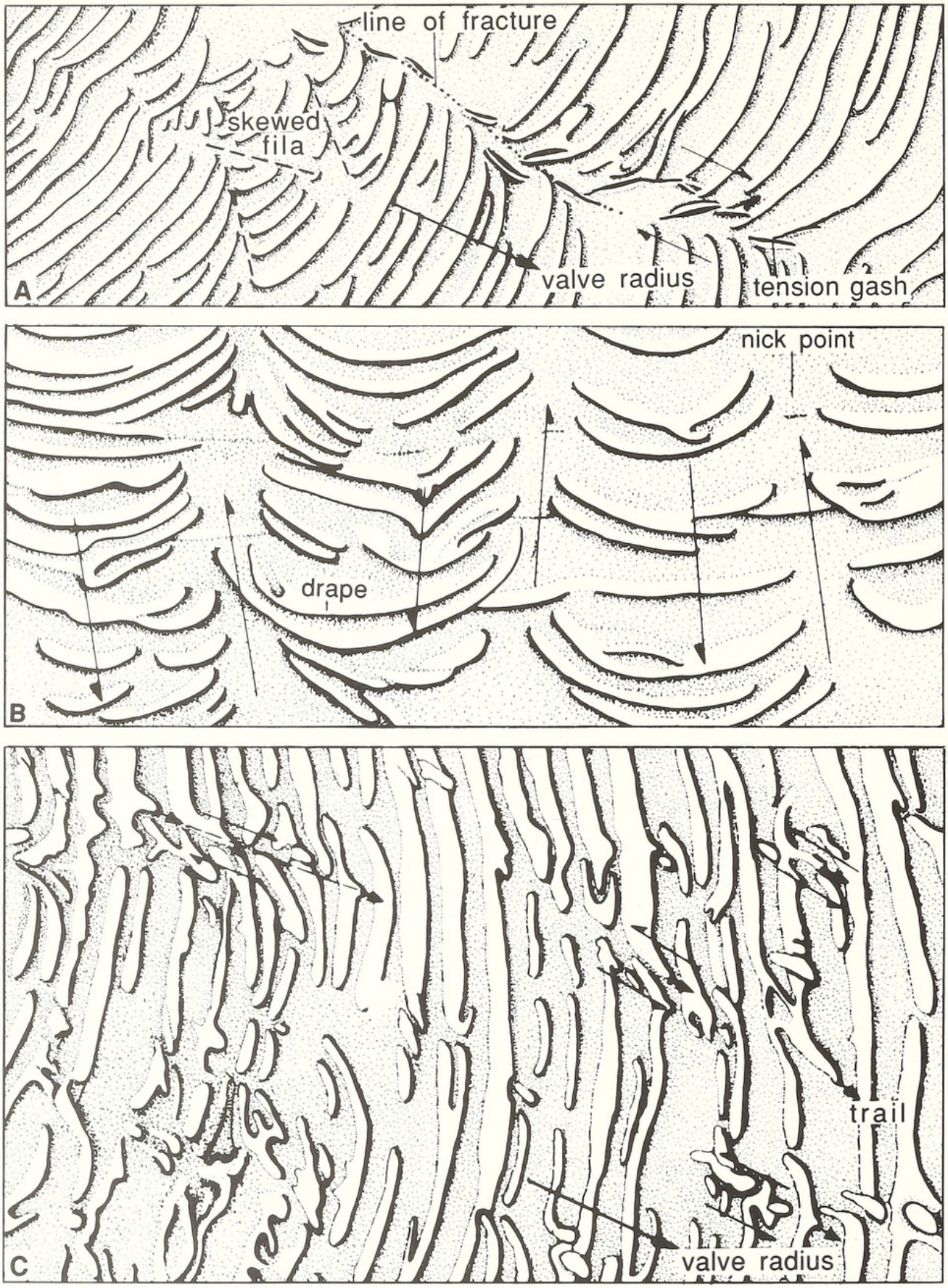

TEXT-FIG. 4. Interpretations of features on the external surfaces of acrotretoid shells. A, breaks and gashes found posteromedianly on a dorsal valve of *Prototreta* sp. interpreted as *in vivo* fracture and malformation (see also Pl. 2, figs 3–4). B, discrete folds interrupting the fila on the posteromedian exterior of a dorsal valve of *Angulotreta postapicalis* (see also Pl. 3, fig 1). C, deformed fila in the median area of a ventral valve of *Prototreta* sp. (see also Pl. 3, fig. 3); the opposing arrows represent inferred stress couples set up during shell secretion.

extending to the margin of the adult valve (Pl. 1, fig. 5). The outline of the dorsal larval shell of 'acrotretroid B' is also indented by the nick points of seven sets of drapes, more or less evenly spaced along a 230 μm arc of the anteromedian edge of the shell (Pl. 2, fig. 6).

The number of nick points along the edge of the larval shell varies with the size of the shell (Text-fig. 5). There is also a tendency for sets to become larger with shell growth, irrespective of their initial size. In *Angulotreta*, the chords of 40 arcuate sets average 17 μm at the edge of three larval shells compared with 38·8 μm for 42 estimates between 200 and 250 μm medioradially of the larval shells. On a dorsal valve of 'acrotretoid B', which is characterized by much larger sets, the average chord widths of 12 and 13 sets at the edge of the larval shell and 350 μm radially from the edge are 38 and 87 μm respectively. In general, however, sets of drapes are less pronounced towards the margins of adult shells. In the dorsal valves of *Torynelasma suecium* Holmer, for example, drapes are well developed within a 350 μm wide arc bordering the larval shell but are lacking from the rest of the juvenile and adult shell.

The most striking aspect of the drapes is the symmetrical disposition of adjacent sets (Text-fig. 4B; Pl. 3, fig. 1). Typically, the backward curving sides of adjacent drapes converge posteriorly at an obtuse angle (nick-point) about a radial axis. In the juvenile part of a dorsal valve of *Angulotreta*, 47 pairs of sets subtend an average angle of 130° within a range of 100 to 150°. Individual drapes on either side of the axis do not always match. They may even branch or anastomose singly and are seldom continuous from one set to another so that two adjacent sets are normally separated by a flat strip of shell, which may be up to 11 μm wide and which only exceptionally bears a few narrow, radial folds.

Variations in the disposition and structure of the drapes do occur, as when they aggregate into parallel-sided rather than arcuate sets (Pl. 3, fig. 2). However, the only significantly different pattern so far seen was found on a ventral valve of a *Prototreta* sp. On this specimen, continuous fila were more frequent and drapes correspondingly less convex. The interspaces of adjacent drapes usually bore rounded folds, up to 4 μm wide, as radially disposed projections from the fila, extending posteromedianly as well as outwardly (Pl. 3, fig. 3). Some of these folds intertwined with one another and with consecutive fila in radially arranged trails (Text-fig. 4C).

Other microarchitectural features of fila, like the pustules ornamenting 'acrotretoid C', are distinguishable from sets of drapes in one important respect: they occur at regular intervals along filar arcs. The pustules of 'acrotretoid C', for example, consist of sharp folds about 2 μm in wavelength (Pl. 3, fig. 5), which plunge posteromedianly and occur at an average interval of 20 μm (for 21 pustules) in alternating arrays along regular fila with a wavelength of about 8 μm between 350 and 400 μm medioradially of the edge of a dorsal larval valve. Sporadic, subdued sets of drapes are impressed on this pattern.

The finer (F_1) folds, occasionally superimposed on fila and drapes, are immediately distinguishable not only by their wavelength which is not more than 1 μm, but also by their disposition. They cut across fila and drapes; but are usually found, more or less radially arranged, in the interspaces of drapes, occasionally in sets of three or four fanning outwards at an acutely divergent angle for up to 30 μm from their point of origin (Pl. 3, fig. 4). This is commonly the disposition of those splaying radially for up to 15 μm from the anterior faces of the pustules ornamenting the fila of 'acrotretoid C' (Pl. 3, fig. 5).

ACROTRETOID SHELL STRUCTURE

The fabric of the acrotretoid shell is already well known mainly through the researches of Poulsen (1971), Rowell (1986), Popov and Ushatinskaya (1986), Ushatinskaya *et al.* (1988) and Holmer (1989). However, in order to understand some of the newly described features of acrotretoid ornamentation, skeletal successions have to be considered further and can be best discussed in the context of a brief review of the variability of the shell structure as presently known. For that purpose, we have founded our skeletal correlation mainly on the published work of one of us (Holmer 1989). That study was primarily concerned with mid-Ordovician species from Sweden. But

the assemblage is diverse and, supplemented by samples of four Cambrian genera, has afforded us information on nearly one-third of all recognized acrotretoid genera. Indeed, the collections at our disposal contained representatives of seven of the nine suprageneric taxa constituting the superfamily. Those not represented, the Linnarssoniinae and Ceratretidae, have been taken as being characterized by two genera with known skeletal structures: *Rhondellina* (Rowell 1986, fig. 1) and *Keyserlingia* (Williams and Rowell 1965, p. H75) respectively. Assuming that the skeletal successions of specimens at our disposal are typical of their respective sub-families and families, the variability of the acrotretoid shell structure may be summarized in a correlation chart as shown in Text-figure 6 (cf. Holmer 1989, fig. 40). It shows that the acrotretoid exoskeleton, so far as we know, may be composed of up to three distinctive biomineralized components described as 'granular', 'columnar' and 'camerate' by Holmer (1989, pp. 31, 43).

The outermost 'granular' layer is invariably present in some part or other of well-preserved shells but rarely continuously so. This patchy occurrence is due to the thinness of the layer which can be entirely lost from surfaces suffering only slight exfoliation. The layer is also commonly recrystallized and may be even more difficult to identify with certainty as a result of the chemical extraction of samples from the rock. However, the outermost layers identified by us as constituents of the acrotretoid skeleton satisfy the following criteria: (1) EDS analyses show that they are composed of calcium phosphate; (2) they bear micromorphic features, like the superficial pits of larval shells, which must have formed during acrotretoid biomineralization although they are not impressed on the underlying skeletal succession; and (3) their interfaces with underlying layers are invariably sharp and generally unconformable (Pl. 3, fig. 6). Such layers are assumed to have originally consisted of the first-formed (i.e. primary) shell.

The primary layer is usually not much more than 1 μm thick even over the larval shell (Pl. 4, fig. 2) where it is pitted with the inferred casts of periostracal vesicles (Biernat and Williams 1970, p. 493). Over the adult shell, the layer varies in thickness from slightly less than 500 nm in *Hisingerella* (Pl. 3, fig. 6) to more than 3 μm in *Torynelasma*. The external skin of the layer consists of closely spaced, elongate granules up to 500 nm long and 200 nm wide, which are orientated with the long axes normal to the surface. In *Torynelasma*, this skin is underlain by closely packed granules, up to 300 nm across and usually without any discernible order and of variable shape. Here and there, as on the ventral pseudointerarea of *Prototreta* and on the ridges between the pits ornamenting the larval shell of *Opsiconidion*, occur closely packed granules, about 100 nm across, with some lineation parallel with, or orthogonal to, the valve margin or the pit edges. We assume that this finely granular state is a relict of the original fabric surviving recrystallization.

The subprimary shell of acrotretoids consists essentially of a stack of laminae, each of which can normally be traced, in some form or other, throughout the skeletal succession internal of its subcircular junction with the primary layer. The laminae usually consist of a mid-region of variably

---

EXPLANATION OF PLATE 2

Fig. 1. *Prototreta* sp. L14900A; enlargement of the external view of a ventral valve showing clusters of densely packed discoidal microstructures and a network of interconnected grooves superimposed on fila, $\times 4100$.

Fig. 2. *Hisingerella billingensis*. Br 128615; view of the partly exfoliated external surface of a ventral valve showing the relationship between the superficial grooves and the partitions of camerate laminae, $\times 1000$.

Figs 3–4. *Prototreta* sp. 3, L14900B; malformed filar drapes on the exterior of a dorsal valve, $\times 350$. 4, L14900B; view of the same valve showing *in vivo* tension gashes and associated minor folding (F_2) seen in the top part of the micrograph, $\times 350$.

Fig. 5. *Angulotreta postapicalis*. L14899C; general view of the external surface of a dorsal valve showing concentric fila, sporadically continuous but usually broken by nick points into sets of drapes, $\times 200$.

Fig. 6. 'Acrotretoid A'. SGU; general view of the dorsal larval shell showing the pitted surface and the margin notched by nick points, $\times 180$.

All scanning electron micrographs.


1

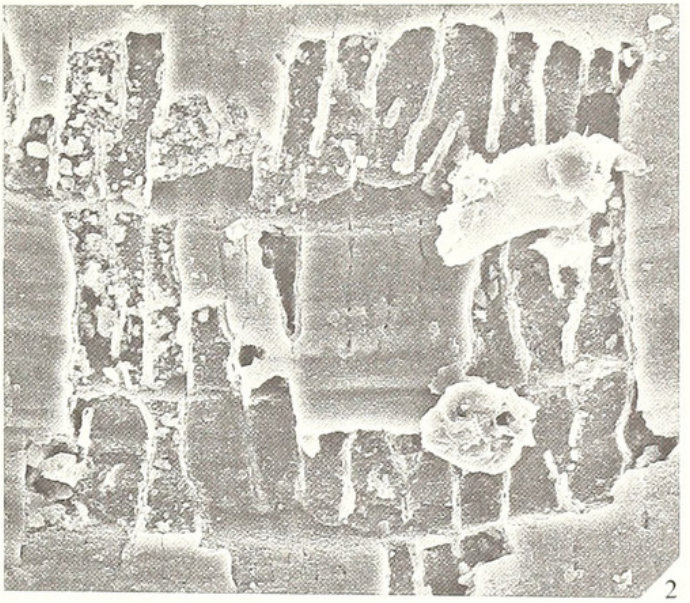
2

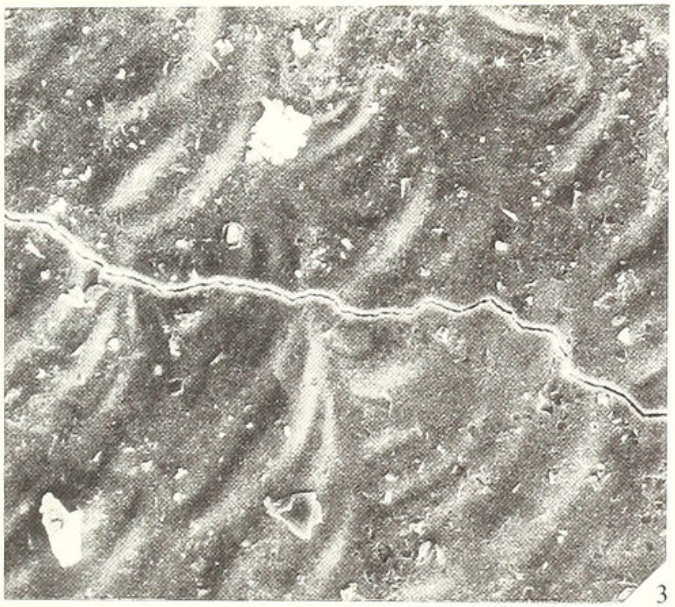
3

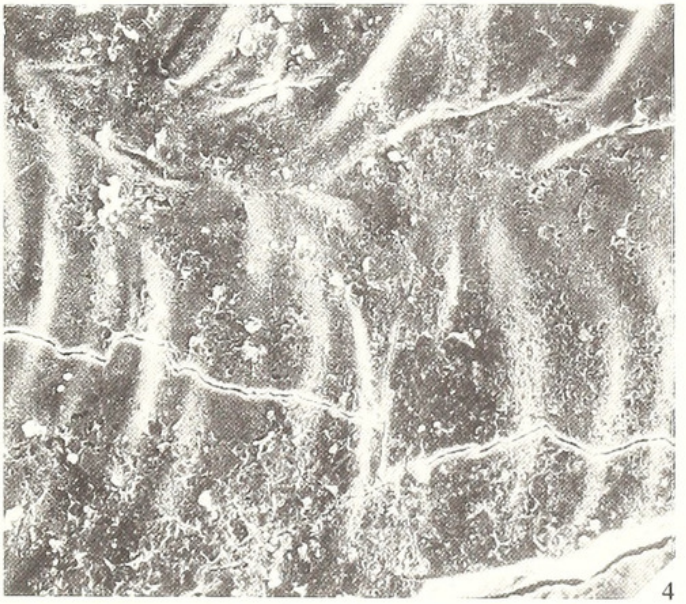
4

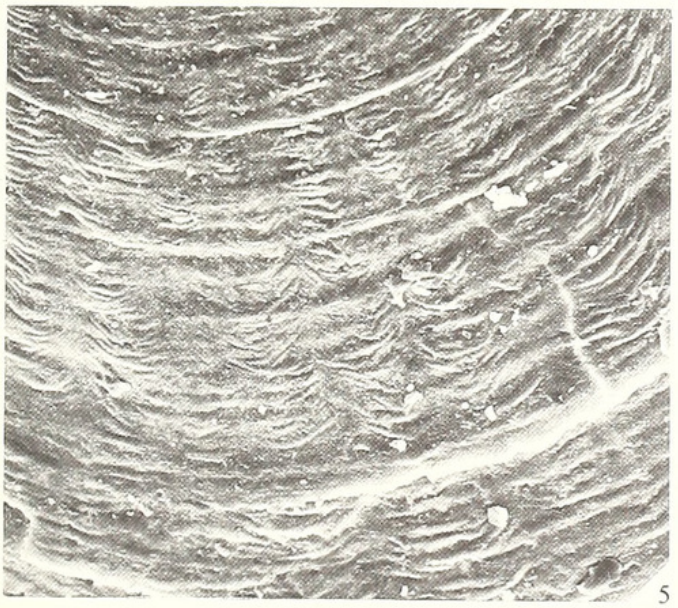
5

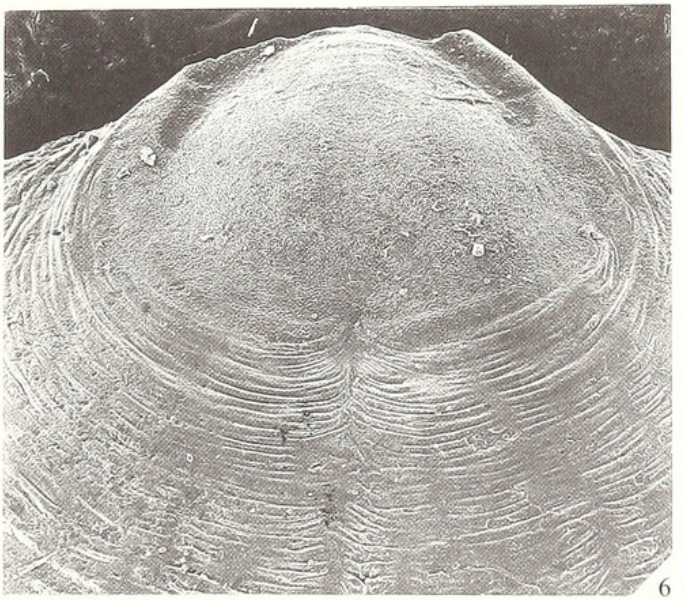
6

WILLIAMS and HOLMER, acrotretoid brachiopods

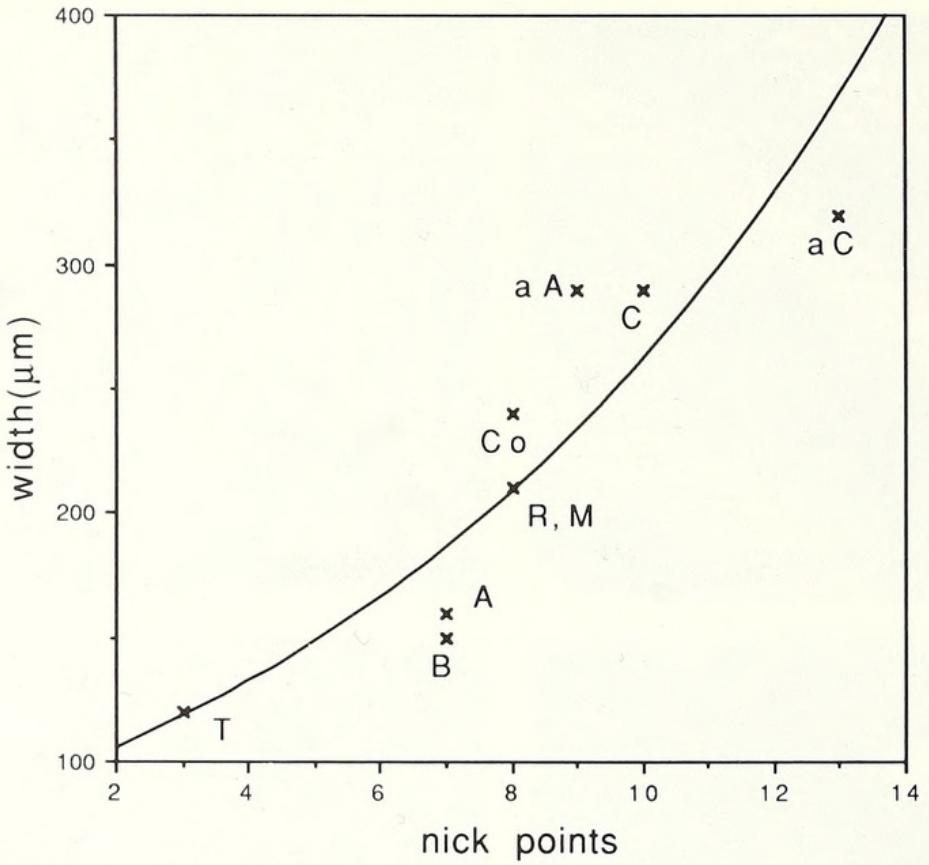

TEXT-FIG. 5. The exponential relationship ($r = 0{\cdot}816$) between the maximum width of the larval shells of nine acrotretoid genera and the number of nick points around the edges of the shells: *Angulotreta* (A); 'acrotretoid A' (aA); *Biernatia* (B); *Conotreta* (Co); *Cyrtonotreta* (C); 'acrotretoid C' (aC); *Myotreta* (M); *Rhinotreta* (R); and *Torynelasma* (T).

developed spaces and two bounding sheets of apatite, the outer and inner lamellae (Text-fig. 7). This arrangement means that a lamina can display, in section, four different surfaces, the external and internal surfaces of both the outer and inner lamellae; and, since each is distinguishable ultrastructurally as well as sequentially, it is important to identify them unambiguously. We shall,

EXPLANATION OF PLATE 3

Fig. 1. *Angulotreta postapicalis*. L14899C; detail of the surface of a dorsal valve showing groups of fila broken by nick points into sets of symmetrical drapes, × 880.

Fig. 2. *Angulotreta triangulata*. L14899D; detail of the external median sector just anterior to the margin of the larval shell (top part of micrograph) of a dorsal valve showing sets of parallel-sided drapes, × 860.

Fig. 3. *Prototreta* sp. L14900B; detail of the exterior of a dorsal valve showing concentric fila frequently interrupted by radially arranged trails extending posteriorly (towards the top right-hand corner) as well as anteriorly, × 750.

Fig. 4. *Angulotreta triangulata*. L14899E; detail of the external surface of a dorsal valve showing fila and fine, linear folds (F_1) running from the bottom right-hand corner to the top edge of the micrograph through the nick points separating two sets of subcentrally placed drapes, × 720.

Fig. 5. 'Acrotretoid C'. Br 133881; detail of the surface of a dorsal valve showing fila pustules and the fine F_1 folds fanning out radially from them, × 1430.

Fig. 6. *Hisingerella tenuis*. Br 128511; detail of external surface of a dorsal valve showing a partly exfoliated arch of primary layer in relation to the underlying, granular camerate secondary layer, × 3800.

All scanning electron micrographs.

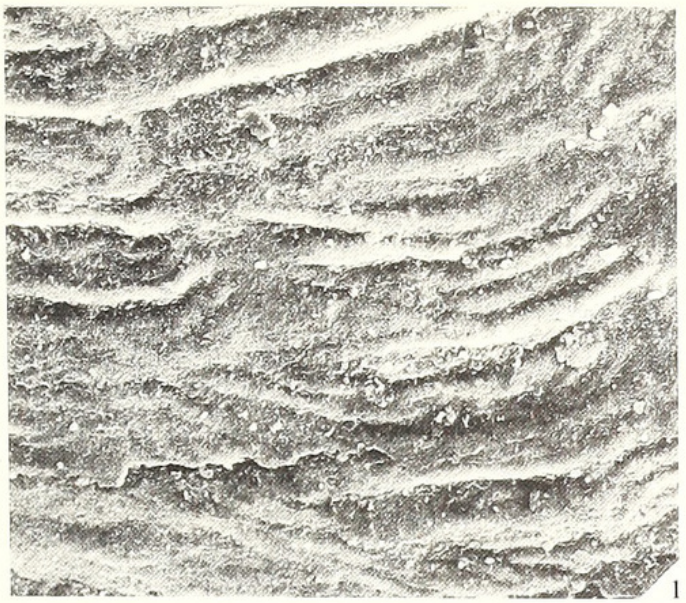
1

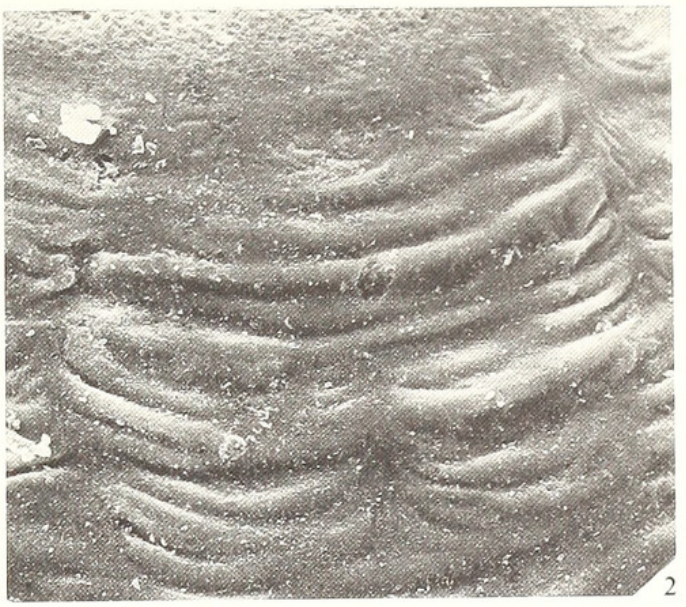
2

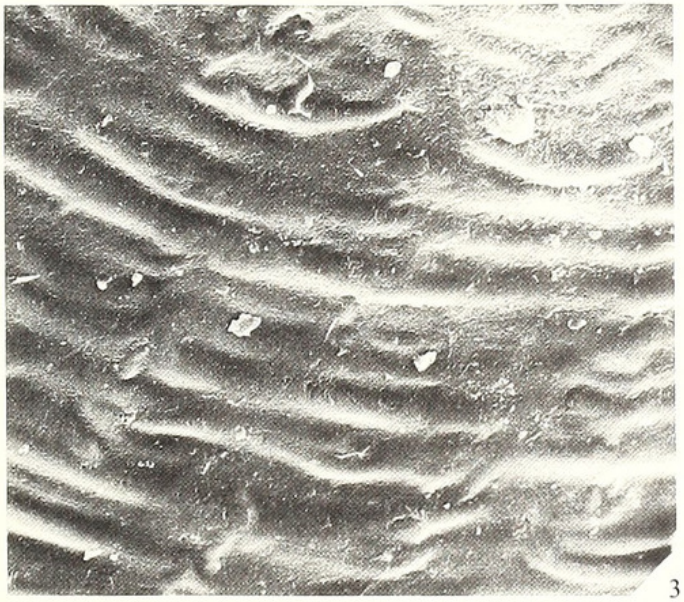
3

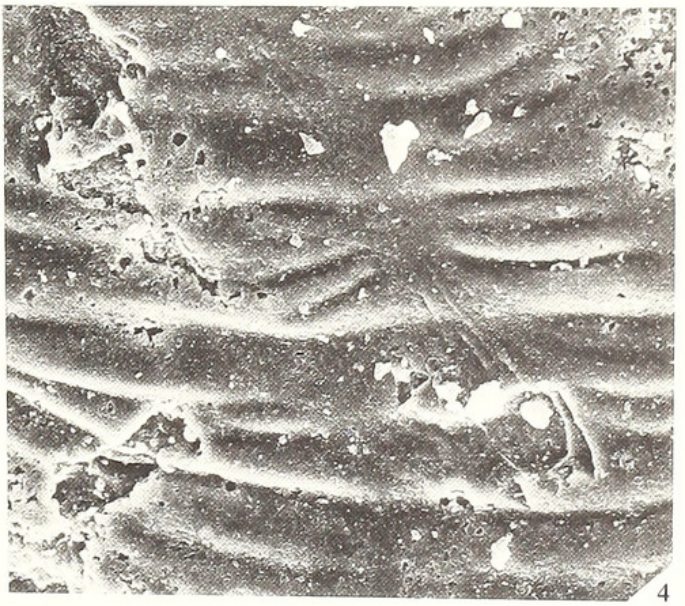
4

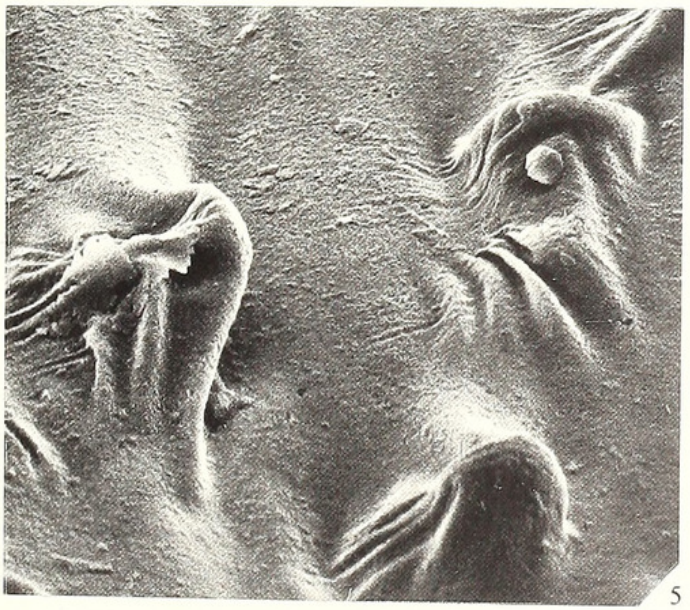
5

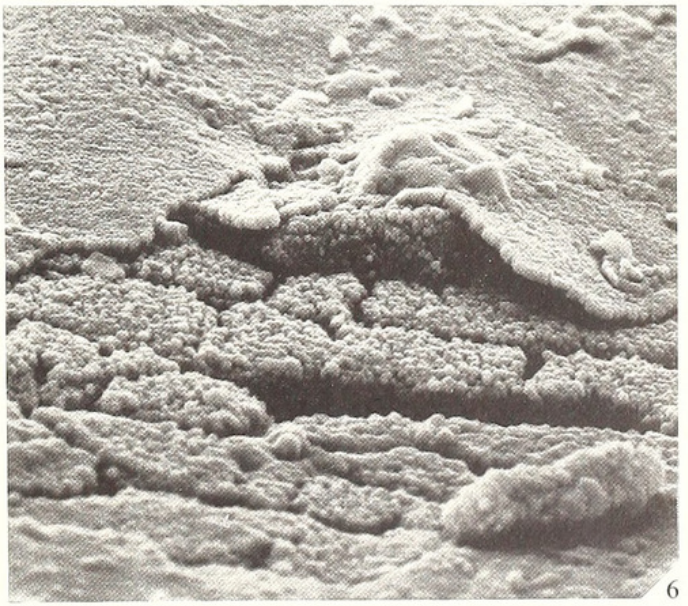
6

WILLIAMS and HOLMER, acrotretoid brachiopods

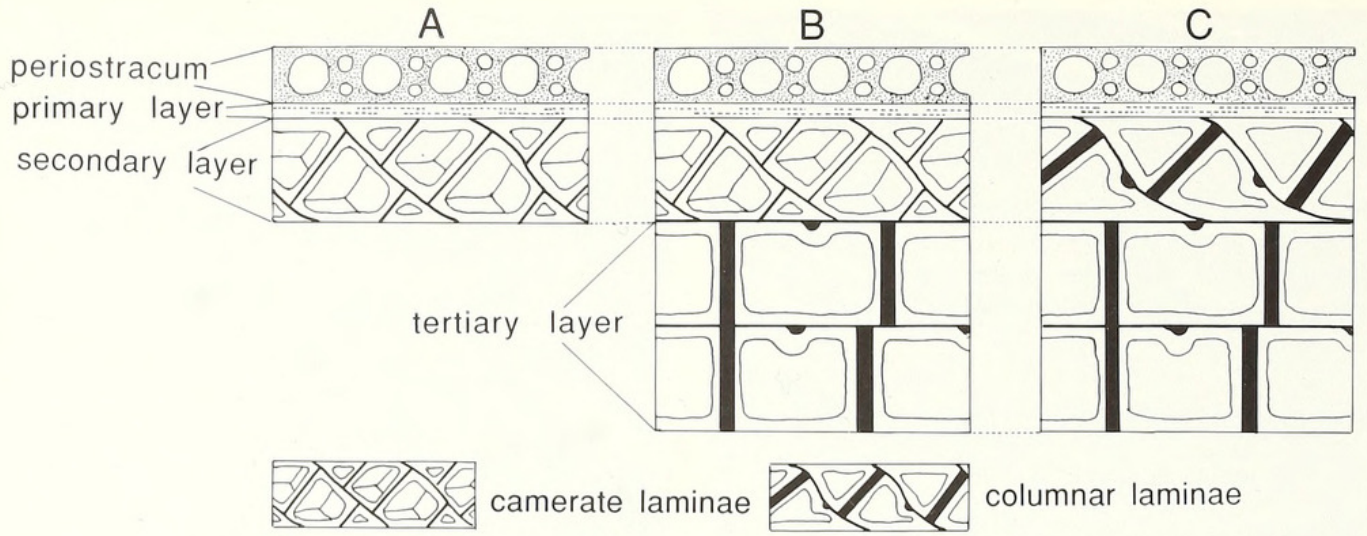

TEXT-FIG. 6. Correlation of the inferred exoskeletal successions of known acrotretoids in the living state as typified by Scaphelasmatinae (A); Acrotretinae and Torynelasmatinae (B); Ephippelasmatinae, Biernatinae and ?Eoconulidae (C).

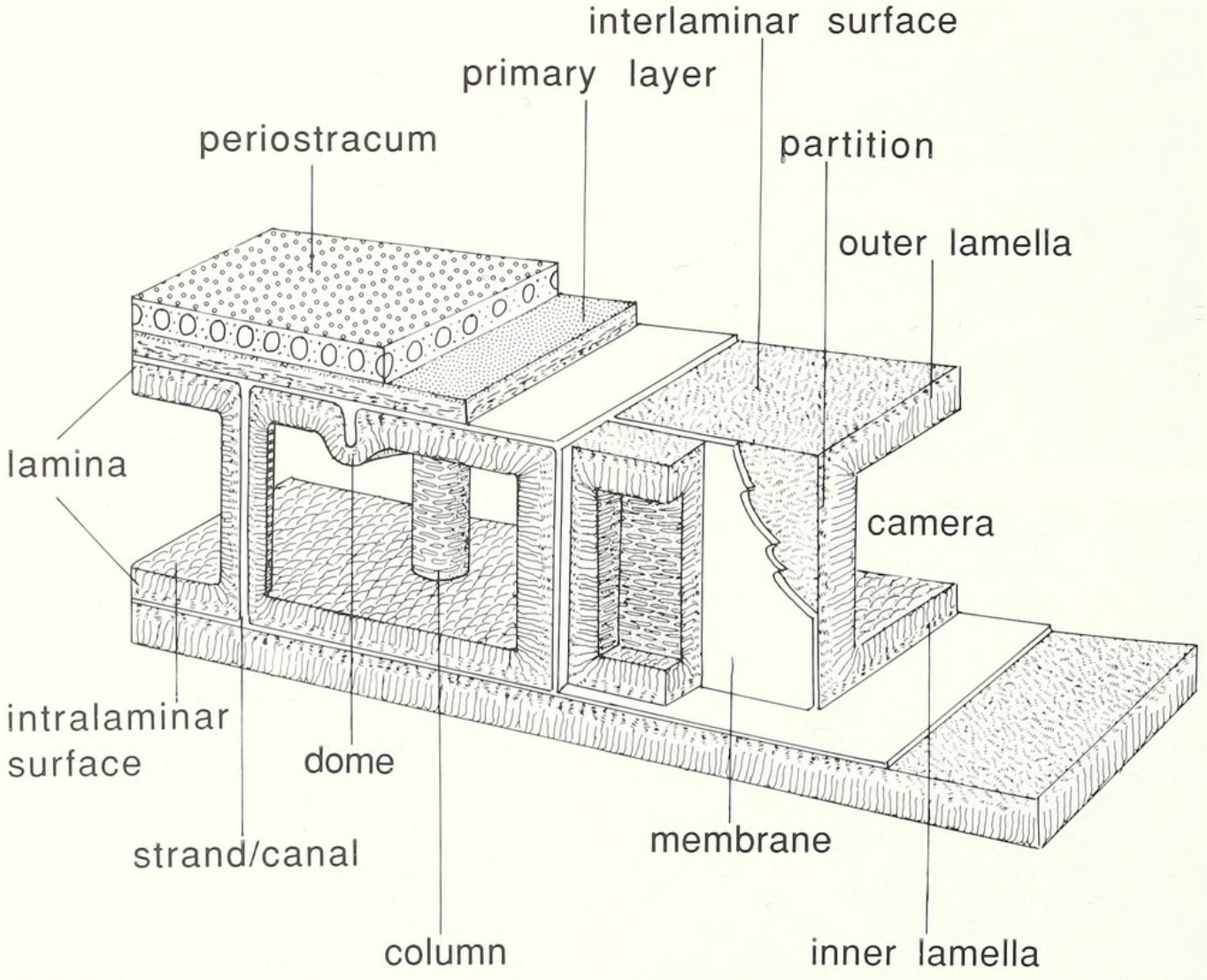

TEXT-FIG. 7. Composite diagram showing the inferred relationships among various biomineral and morphological components of the shell of living acrotretoids.

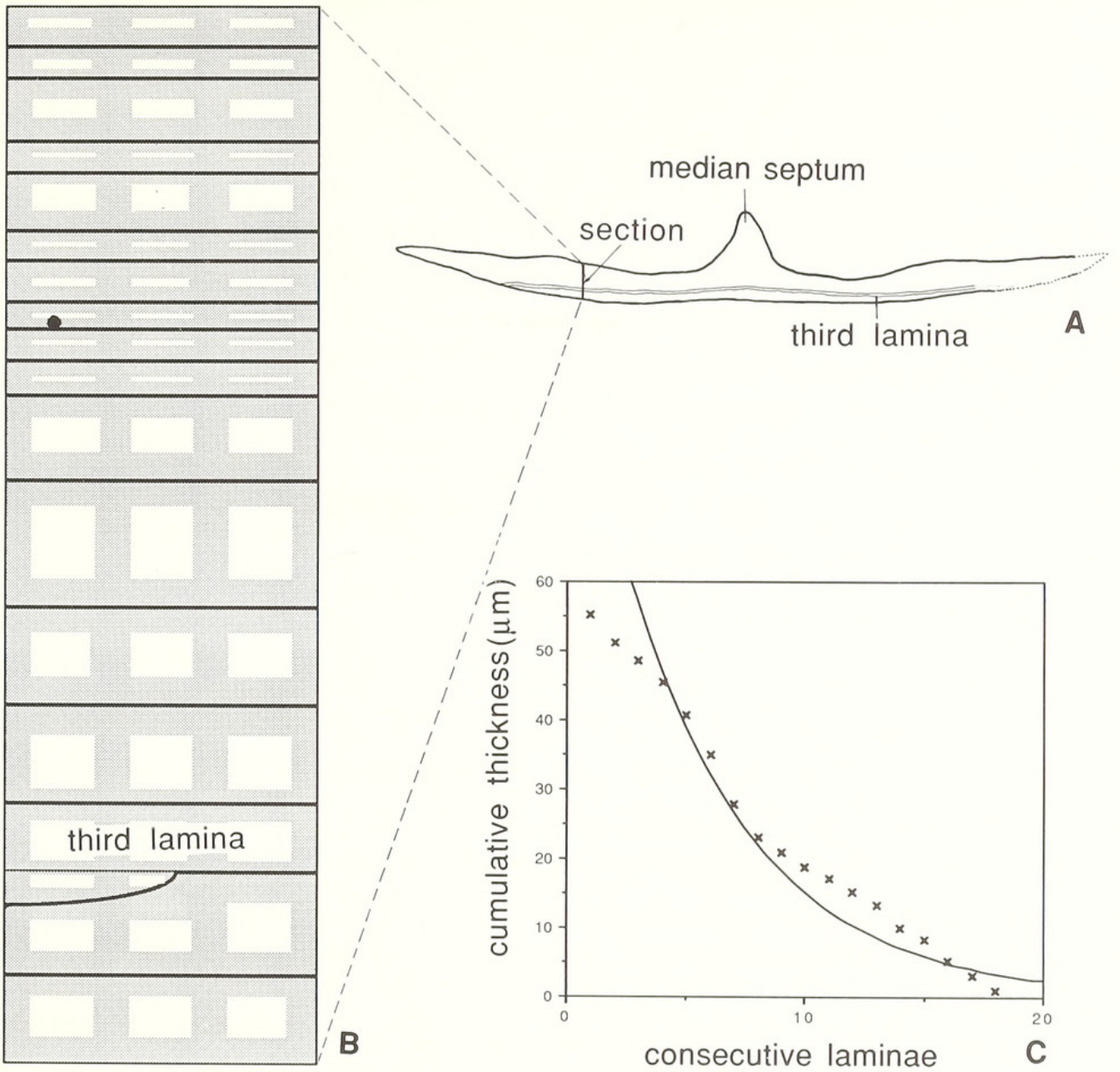

TEXT-FIG. 8. Stylized representation (B) of a strip section through the dorsal valve of *Angulotreta postapicalis* (A) with an exponential analysis (C) ($r = 0{\cdot}854$) of the cumulative thickness of the consecutive laminae from the interior outwards; the third lamina inwards from the exterior (as indicated in B) was traced continuously through the section at A.

therefore, refer to the four surfaces as the interlaminar and intralaminar surfaces of the outer lamella and the intralaminar and interlaminar surfaces of the inner lamella from the exterior to the interior consecutively.

A lamina is typically thicker at the margin than medianly. One lamina, exposed in a fracture section roughly along the maximum width of a dorsal valve of *Angulotreta* (Text-fig. 8), was traced from its left margin of origin for 1·02 mm to the right lateral part of the valve where it was probably not more than 90 μm short of its right margin. The maximum thickness (12 μm), as measured between its inner and outer interlaminar surfaces, was at the margin; whereas the minimum thickness (6·5 μm) was in the mid-region beneath the root of the dorsal septum. Since successive lamina are progressively more distant from their respective margins, they tend to become thinner

internally in any given section. However, variations in secretory rates, reflecting the differential growth of morphological features as well as the intervention of environmental factors, would have given rise to anomalies. Thus in Text-figure 8, which shows the disposition of 18 laminae in a strip section of a dorsal valve of *Angulotreta*, the thicknesses vary from 7·9 μm to 1·7 μm and, while reduction is exponential towards the interior, the progression is not perfect ($r = 0{\cdot}854$).

More extreme variations in laminar thicknesses usually attend the development of strong fila. In *Myotreta dalecarlica* Holmer (Holmer 1989, fig. 31), the margin of a lamina, which deflected outwards at about 20° to the floor of the valve, was 6·8 μm thick but attenuated rapidly to less than 500 nm within 25 μm of the laminar edge. Inwardly the lamina was no longer distinguishable as it merged with a break in the shell succession, which underlay all such marginal wedges. The same kind of laminae can, however, occur in acrotretoids lacking fila. Thus, in a specimen of the smooth *Biernatia holmi* Holmer (Holmer 1989, fig. 34) the laminar margins deflect outwardly by as much as 35° and the thickness diminishes from a maximum of 2·5 μm at the external surface to about 250 nm within 14 μm of the shell exterior. In effect, such valves are composed of successive ring-like laminae which are wedge-shaped in radial section and underlain by a transgressive series of more or less horizontal laminae which are the isochronous correlatives of more distal, younger laminar wedges.

Apart from reflecting variations in the rates of laminar secretion, the cumulative thickness of the acrotretoid shell was also possibly affected by resorption and certainly by the intercalation of impersistent laminae. Indeed, the margins of acrotretoid valves are usually thickened in adult stages of growth by the intercalation of peripheral ring-like laminae which die out medianly to appear as discontinuous wedges in radial section. Thus, the 0·25 mm marginal zone of a dorsal valve of *Conotreta*? *siljanensis* Holmer, with a maximum width of 2·12 mm, is made up mainly of discontinuous laminae, cumulatively 6 μm thick and inclined at up to 20° to the external surface of the valve (Holmer 1989, fig. 27; Text-fig. 9).

In contrast, impersistent laminae appear to be rare components of the floors of the shell and, in *Angulotreta* at least, are seldom more than 50 μm wide. They are, however, relatively common in the fabric of outgrowths arising from the floor of a valve, where they supplement thickened zones of the more persistent laminae. In the median septum of the dorsal valve *C.*? *siljanensis*, referred to above, the root of the structure is an intercalated, prismatic lamina with an inwardly directed crest. In the rest of the septum, thickening was exponential (Text-fig. 9) giving rise to narrow overlapping laminae which are steeply concavo-convex in section. Eight of these were intercalated and only 66 μm lateral of the septum, the total number of laminae was reduced to nine with an average thickness of 2·7 μm.

The interlaminar surfaces bounding individual laminae are immediately identifiable in natural or polished sections as sharp linear breaks (Pl. 5, figs 1–2, 6). Contiguous laminae are usually separated by gaps up to 500 nm, but most commonly less than 250 nm, wide yet seldom so close as to obscure their separation. Their micromorphology is best studied in oblique fracture sections or in exfoliated inliers within the primary layer, where the relationships between interlaminar and intralaminar surfaces are least confusing. The differences, however, are very strong and reflect contrasting modes of secretion.

The surfaces exposed within inliers of primary shell are very fine granular or even discreetly tuberculate with units up to 250 nm or so in size (Pl. 4, fig. 1). They may be contoured with fine terraces about 500 nm apart, which are presumably traces of banding within the lamellae, gently dipping postero-radially relative to the interface with the primary layer (Pl. 4, fig. 3). The surfaces are also indented by cuneiform or subcircular pits, averaging about 150 nm and 480 nm in diameter respectively. They are especially well developed immediately below the interface with the primary layer where they can be densely distributed at intervals of less than 1 μm. Exfoliation of the lamellar banding reveals that the pits are mostly superficial since they become sporadically distributed inwardly of the interface.

The interlaminar surfaces exposed internally are also finely granular with a grain size of about 150 nm and pitted with circular depressions and canal openings, usually about 500 nm in diameter

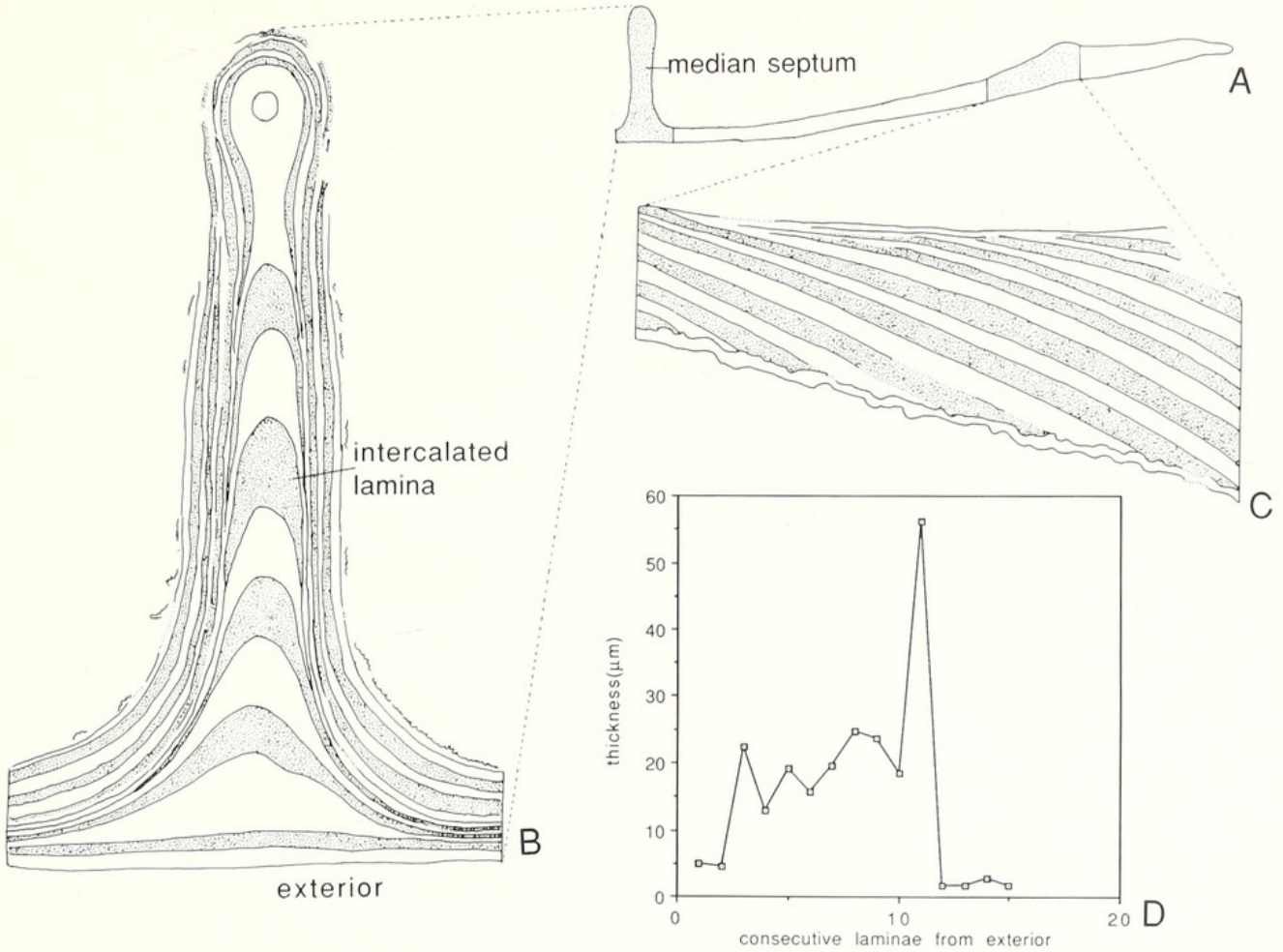

TEXT-FIG. 9. Outline section of part of a dorsal valve of *Conotreta*? *siljanensis* (A) showing the locations of detailed drawings featuring the secondary laminae (alternately shaded) of the median septum (B) and an intramarginal zone (C); the graph (D) is a plot of the maximum thicknesses of consecutive laminae from the exterior to the tip of the median septum.

but more rarely approaching 1 μm (Pl. 4, figs 4–5). Occasionally, however, as in *Linnarssonella girtyi*, a surface may bear sets of shallow grooves or ridges, about 1·2 μm wide and 10 μm long in a close-packed hexagonal network over areas of 0·05 mm^2 or more (Pl. 4, fig. 6). The hexagonal areas, which vary in maximum length from 8 μm to 14·5 μm, are slightly raised and indented by cuneiform and subcircular depressions comparable in size with those seen on the interface with the primary layer. It should be noted that the intralaminar surfaces of the outer lamellae of *L. girtyi* are also ornamented by the same hexagonal pattern although the boundaries are usually ridges rather than grooves and the floors of the hexagons may be packed with low domes up to 2 μm in diameter (Pl. 4, fig. 6). More significantly, hexagonal networks of low ridges found intramarginally in dorsal valves of *Cyrtonotreta* and *Conotreta* can be shown to be continuous with identically disposed partitions in the underlying camerate laminae.

The decreasing thickness of a lamina, medially of its junction with the primary layer, is a function of the narrowing space between its bounding lamellae. The lamellae also vary in thickness, but not significantly, in any given section. Thus, the mean thicknesses (with standard deviations) of the 18 pairs of outer and inner lamellae in the *Angulotreta* succession shown in Text-figure 8, were 0·923 μm (0·318) and 0·947 μm (0·32), respectively.

The apatite of the lamellae is usually recrystallized as closely stacked pinacoidal plates about 80 nm thick or as acicular crystallites up to 170 nm wide (Pl. 5, figs 1–2). Both forms are disposed

normal to the interlaminar surfaces. Less frequently, lamellae consist of mosaics of granules, up to 250 nm across and occasionally arranged in fine bands about 150 nm thick, which are assumed to be relicts of the original fabric (Pl. 5, fig. 6).

The intralaminar surfaces, enclosing the variably developed spaces between pairs of outer and inner lamellae, differ from interlaminar ones in two respects. First, they are much rougher topographically, mainly through features of recrystallization, like serrated edges of stacked pinacoids, erect bipyramidal prisms and so on. However, there are also more rarely occurring patches of granular mosaics, with granules, each up to 300 nm across and dispersed depressions 1·5 μm or so in diameter, which could well represent the original fabric (Pl. 5, fig. 6). Secondly, paired intralaminar surfaces are almost invariably connected by apatitic columns or partitions while domes of the same composition also occur on the outer of the surfaces subtending columns (Pl. 5, fig. 3; Pl. 7, fig. 2). As domes are associated with columns and may be formed before them, they will be described first.

Domes vary in size and density of distribution. They are normally hemispherical shape but may be flattened or elongated into cylindroid outgrowths with rounded free ends occasionally dimpled by a central depression less than 200 nm in diameter (Pl. 5, fig. 6; Pl. 6, fig. 1). Their diameters vary from 2 μm to more than 5 μm, with an average of 2·6 μm for a group of 20 (range 1·9–3·2 μm) or an intralaminar surface near the anteromedian margin of a ventral valve of *Angulotreta*. The domes are densely packed with up to 45 occurring in 400 μm^2, some in various stages of amalgamation (Pl. 5, fig. 4). However, between 8 to 12 were counted in equal areas of the apical region of the valve.

The ultrastructure of the domes, irrespective of size, is complex, presumably as a result of recrystallization. They appear to have a core of apatitic granules up to 700 nm across; but well-preserved domes are covered with curved, overlapping plates less than 100 nm thick which may be pinacoidal (Pl. 5, fig. 5).

The apatitic columns connecting paired intralaminar surfaces are comparable in diameter and distribution with the domes, especially the more dispersed ones. In the ventral apical region of *Angulotreta*, for example, the bases of nine columns as well as three domes were counted in an area of 400 μm^2. The columns are uniformly cylindrical with diameters ranging from 1·5 μm to over 5 μm, although they tend to be less variable within consecutive laminae in a strip section. The means (not standard deviations) of the diameters of 20 columns and of the widths of 20 intercolumnar spaces were 2·26 μm (0·289) and 3·37 μm (1·679) respectively. Other noteworthy features of the intralaminar columns include: their tendency to bend especially between the lamellae of internal structures like septa (Pl. 5, fig. 3); the sporadic development of a few shallow nodes which impart a slightly beaded appearance (Pl. 6, fig. 3); and their frequent continuity from one lamina to the next (Pl. 5, figs 1, 3). In *Angulotreta* it is not uncommon to find a column running for 30 μm or more through three laminae to end in a dome without any apparent break other than interlaminar slots.

In *Angulotreta*, hexagonal prisms and bipyramids of apatite of varying sizes are frequently found

---

EXPLANATION OF PLATE 4

Figs 1–5. *Angulotreta postapicalis*. 1, L14899F; detail of the external surface of a dorsal valve showing an inlier of secondary shell beneath the superficial primary layer, ×750. 2, L14899D; external detail of a partly exfoliated dorsal larval shell showing the pitted nature of the primary layer, ×830. 3, L14899G; detail of secondary laminar surfaces immediately beneath the interface with the primary layer showing fine terracing and cuneiform or subcircular pits, ×4150. 4, L14901A; oblique fracture surface of a ventral valve showing a succession of columnar laminae with a well-exposed, comparatively smooth interlaminar surface, ×1100. 5, L14901B; detail of an interlaminar surface within a fracture section of a ventral valve showing the finely granular texture, pits and rare domes, ×5400.

Fig. 6. *Linnarssonella girtyi*. L14897; detail of an intralaminar surface (with a smoother interlaminar surface along the left-hand edge) of a ventral valve showing the close-packed hexagonal network of ridges delineating areas packed with low domes, ×750.

All scanning electron micrographs.

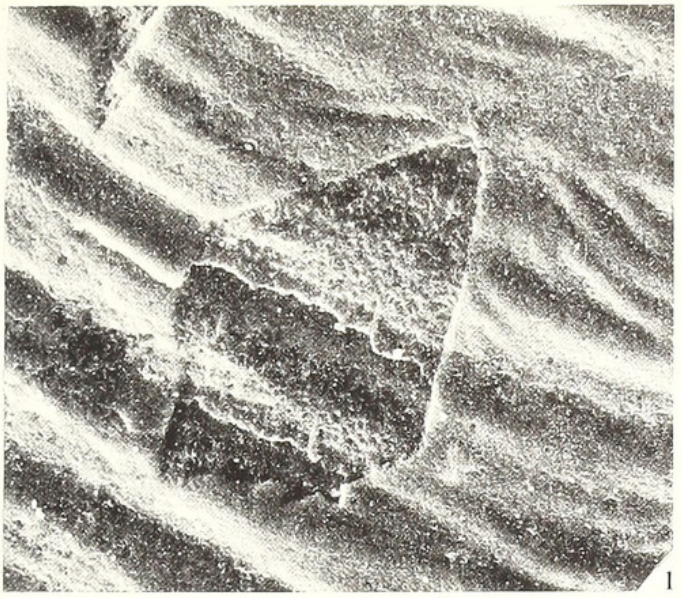
1

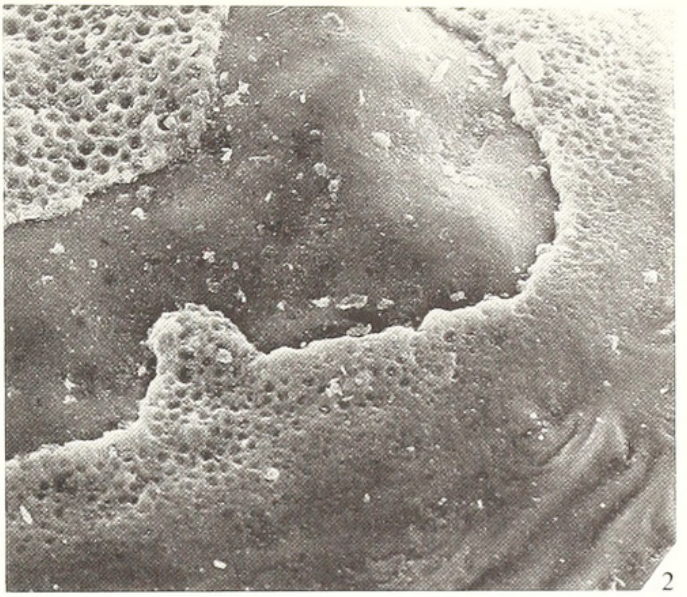
2

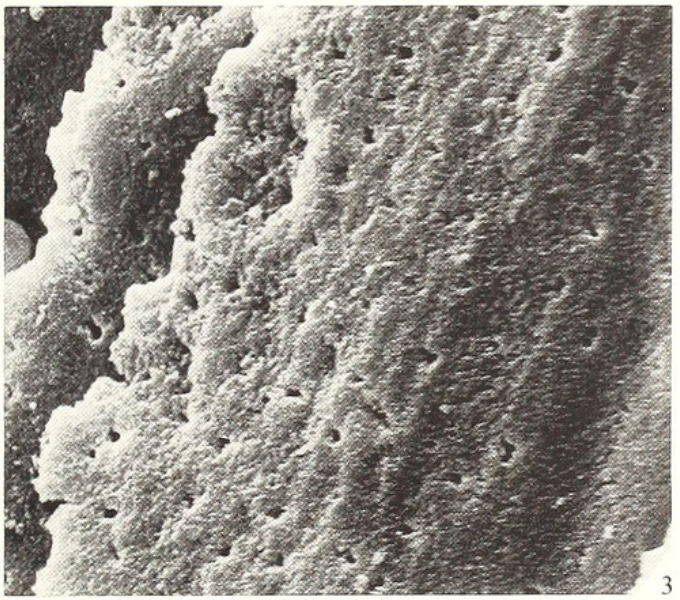
3

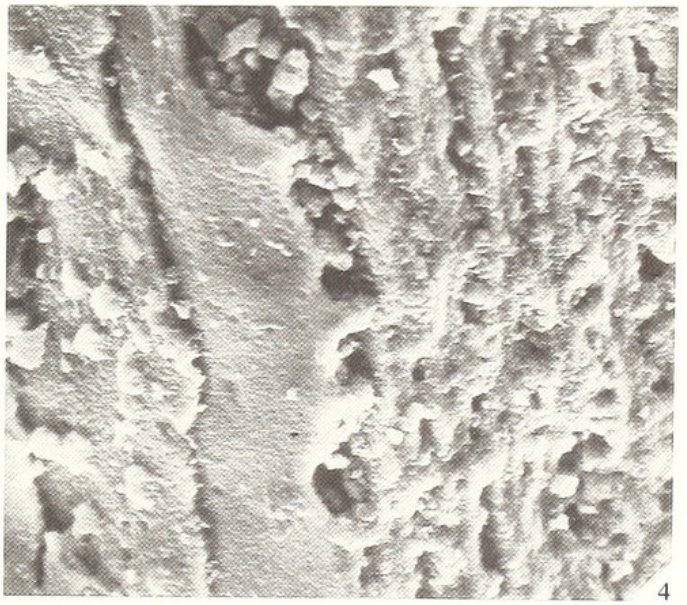
4

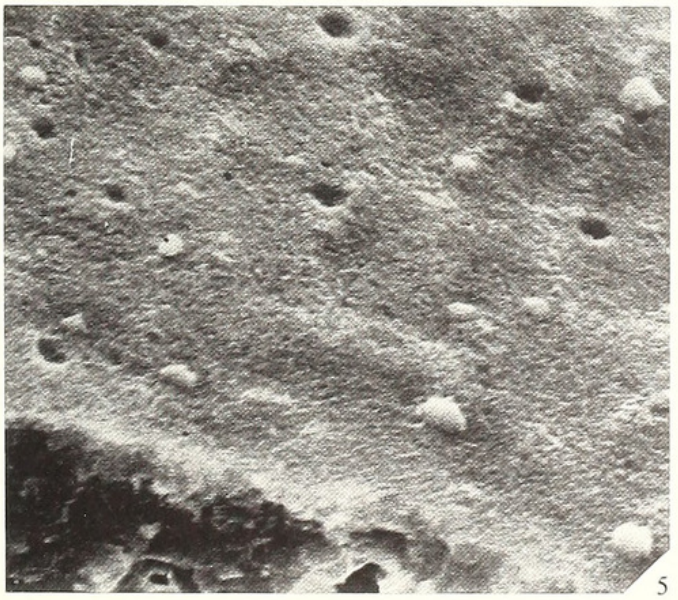
5

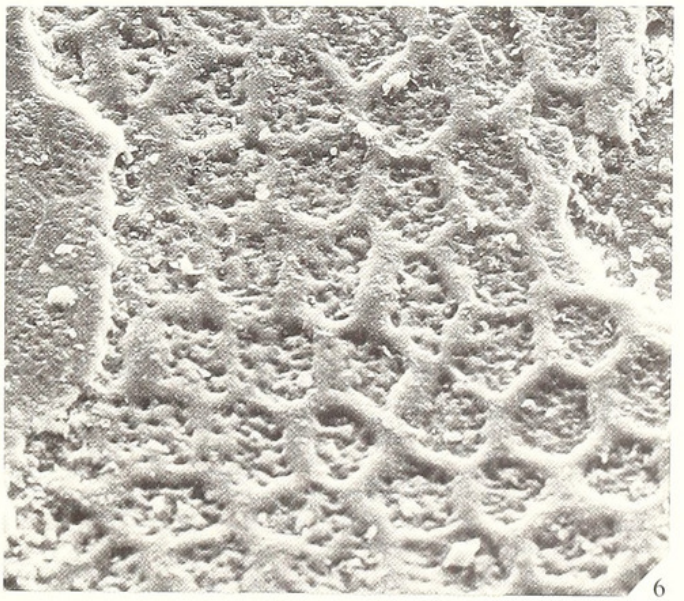
6

adhering to the columns or in clusters within the intercolumnar spaces (Pl. 6, fig. 4). These products of recrystallization do not, however, entirely obscure the characteristic fabric of a column. Its external surface is a comparatively smooth mosaic of interlocking granules, 300–500 nm across. Transverse fractures through the columns show that these granules are the bases of acutely pyramidal crystallites (Pl. 6, figs 5–6) up to 1 μm long, disposed centripetally to delineate an axial canal with a diameter of about one-quarter that of the column. The canals may be partly filled with recrystallized apatite but exposures of empty segments show that their walls are also comparatively smooth (Holmer 1989, fig. 23D).

The other structures, forming a series of junctions between paired lamellae, are the apatitic partitions which divide the intralaminar spaces into camerae. They are shown in exceptionally well-preserved interiors of *Hisingerella tenuis*, along the entire valve margin to the posteromedian pseudointerarea (Pl. 7, figs 1–2). Exfoliation of patches of the primary layer reveals that the camerate partitions underlie the earlier described grooves occasionally found on the primary layer (Pl. 2, fig. 2). Accordingly, the partitions, like the network of grooves, are typically disposed in parallel-sided, radial arrays, divided into variable segments by transverse, oblique or lobate offshoots. Indeed, there is an even closer relationship for the grooves can be continuous with medial slots, seldom more than 200 nm wide, which divide the partitions into paired walls (Pl. 7, fig. 4). As a result, each camera is typically a space enclosed by a continuous layer of apatite consisting of portions of outer and inner lamellae and the walls of the confining partitions. Such a structure is ideally a discrete unit separated from its neighbours by the breaks between the interlaminar surfaces of the lamellae and the slots between the intrapartition surfaces of the walls (Text-fig. 7).

The intrapartition surfaces between adjacent camerae are finely granular with a constituent size of 100–200 nm in *Hisingerella*. In this respect, they are comparable with interlamellar surfaces and easily distinguishable from the coarsely granular interpartition surfaces. The texture of the interpartition surfaces reflects the crystalline structure of the camerate walls which are usually composed of acicular apatite about 1 μm long and 170 nm wide as in *Prototreta alternata* (Meek) (Holmer 1989, fig. 22), but can also consist of elongate granules, about 500 nm long and 200 nm wide, as in *Hisingerella billingensis* Holmer.

The relationships between intralaminar columns, domes and partitions are complex and have yet to be satisfactorily resolved. Despite evidence in *Angulotreta* of the amalgamation of domes, exceptionally into low ridges up to 13 μm long and 1·5 μm wide, no well-ordered linear arrangements comparable with partition patterns have yet been seen. On the other hand, a partly exfoliated interior of *Scaphelasma mica* Popov shows radially subparallel partitions, at intervals of about 3 μm, becoming beaded, then dividing into trails of dome-like bodies up to 2 μm in diameter before giving way posteromedianly to densely distributed domes, some of which are amalgamated into haphazardly branched configurations (Pl. 7, fig. 3).

EXPLANATION OF PLATE 5

Figs 1–6. *Angulotreta postapicalis*. 1, F14902A; detail of recrystallized columnar laminae of a dorsal valve with exterior beyond the top left-hand corner of micrograph, ×3500. 2, F14902A; detail of narrower laminae internal of those shown in figure 1 with domes on the outer intralaminar surfaces, ×4150. 3, F14902A; general view of a fracture section through the apical region of a ventral valve (with the interior towards the bottom right-hand corner) showing the secondary layer of columnar laminae, ×830. 4, F14902B; general view of interior of ventral valve showing a smooth interlaminar surface along the bottom of the micrograph and intralaminar surfaces with domes, ×1000. 5, F14902B; detail of the curved plates covering tops of domes on an inwardly facing intralaminar surface of a dorsal valve, ×7000. 6, F14902C; detail of fractured outer lamella of a ventral valve showing the granular nature of the intralaminar surface, the cleaved structure of the domes and the interlaminar slot between the outer lamella and the inner lamella of the adjacent external lamina (along the left-hand side of the micrograph), ×7000.

All scanning electron micrographs.

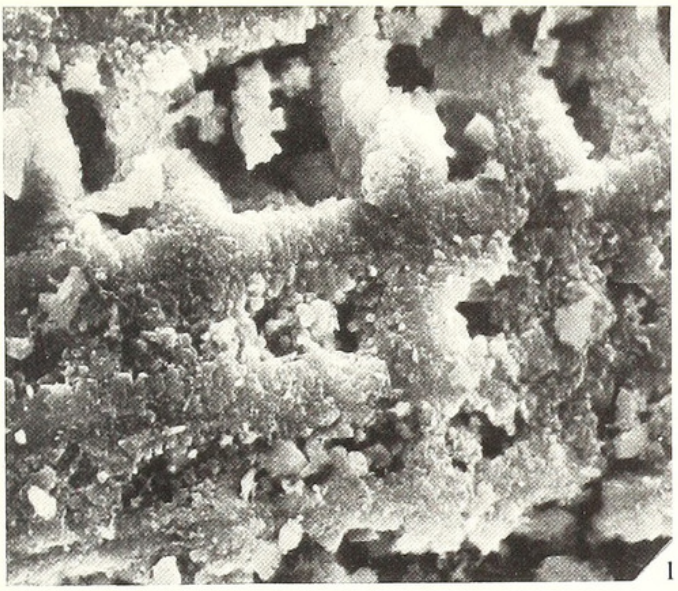
1

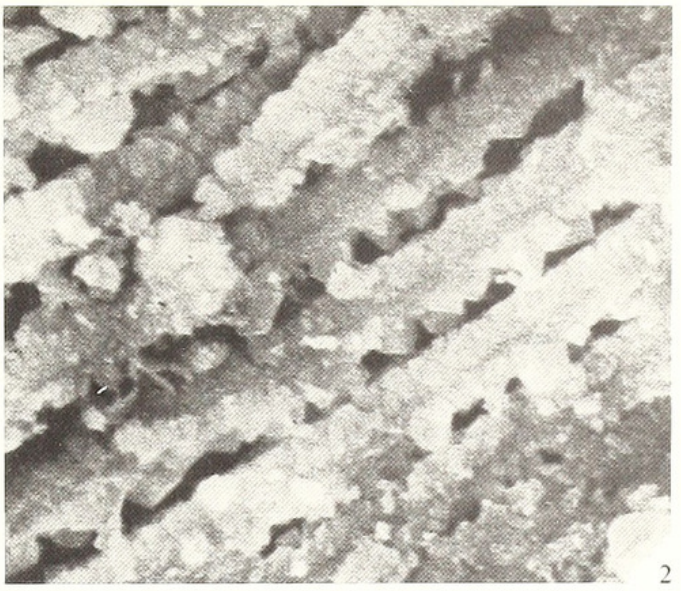
2

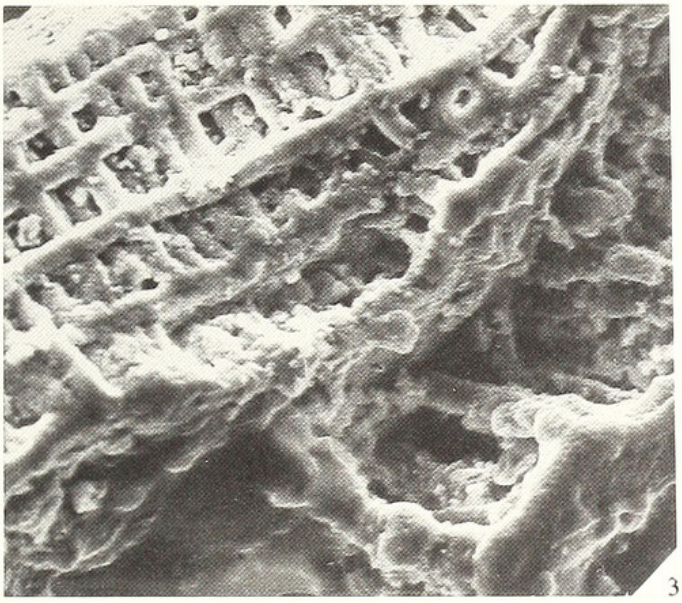
3

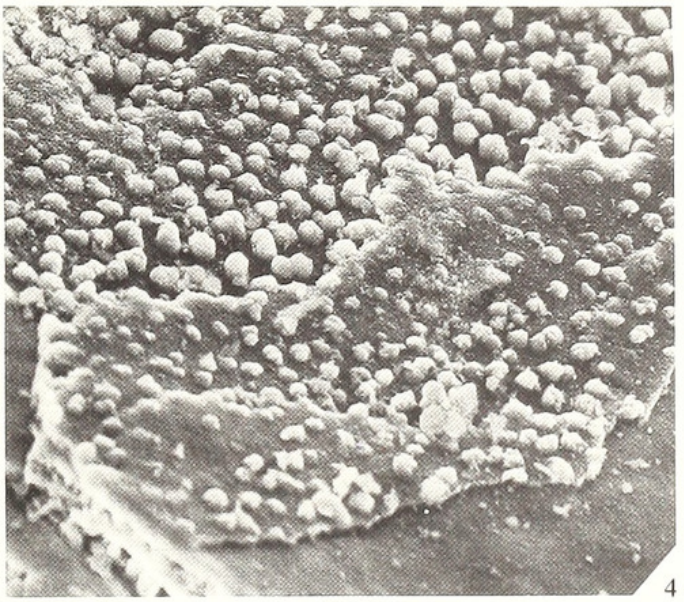
4

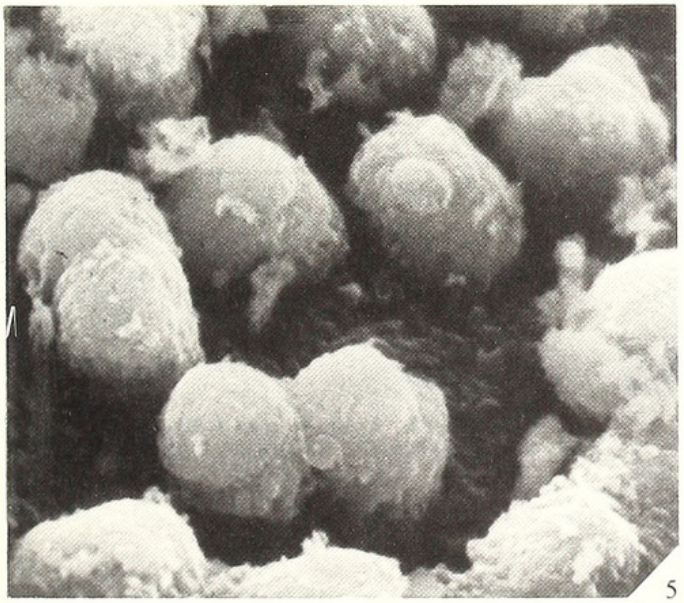
5

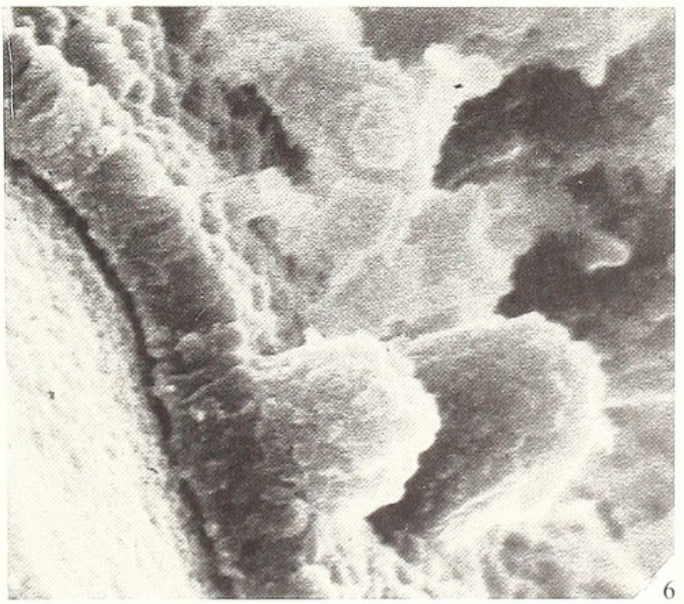
6

So far as shell successions are concerned, it is noteworthy that the secondary layer may consist of camerate or columnar laminae but that a tertiary layer, when present, is invariably columnar (Text-fig. 6).

Acrotretoid laminae normally contain columns or partitions throughout their spread, but intralaminar spaces are occasionally so reduced that such features are no longer distinguishable. The structural consequences of this lamellar closure are seen in three consecutive columnar laminae (about the fifth to the seventh from the exterior) in the posteromedian succession of a ventral valve of *Angulotreta*. As the intralaminar spaces narrowed, they become filled with a granular mesh of apatite riddled with slots and holes, up to 450 nm in diameter, which are clearly sections of anastomosing passages through an apatitic substrate (Pl. 6, fig. 2). The same kind of porous apatite, the cryptocrystalline calcium phosphate (CCP) of Holmer (1989, p. 41), fills the intralaminar spaces of many other acrotretoids including *Hisingerella*. The granular mesh is instantly distinguishable from the prisms and pinacoids of recrystallization and is believed to be an original component of the biomineral succession.

INFERRED SKELETAL SUCCESSIONS OF LIVING ACROTRETOIDS

Acrotretoid periostracum

In living lingulid brachiopods, the chitinophosphatic shell is bounded by a periostracum secreted by a band of vesicular cells forming the outer mantle lobe and much of the inwardly facing periostracal lobe. In all brachiopods, so far as is known, vesicular cells have a characteristic parallel-sided, elongate shape, easily distinguishable from the equidimensional outline of the typical cuboidal epithelial cell of the mantle proper (Williams 1977, p. 117). In *Glottidia pyramidata* (Stimpson), for example, vesicular cells are seldom more than 1·5 μm wide but may be up to 15 μm long. Another point of special interest is that the introverted periostracal margin of living lingulids is underlain distally by a thin coat of apatite, according to back scatter analysis of sections of dried *Glottidia*. The degree of introversion may have been accentuated by the dried state of the specimen, but the observation is still apposite. The first coat of apatite, as well as the overlying periostracum proper, is sufficiently flexible to be conveyed continuously around the outer mantle lobe and added to the external edge of a growing valve.

The secretory regimes of other living chitinophosphatic inarticulates, the discinids, which are actually more closely related to the acrotretoids, are presently being investigated by one of us (A. W.) but can reasonably be deduced in their generality from Blochmann's drawing (1900, pl. IX, 17) of the mantle edge of *Discinisca lamellosa* (Broderip). The genus almost certainly has a well-defined outer mantle lobe with a band of elongate vesicular cells, although their relationship with other cell bands is unknown. A relevant observation, which has already been made on critical point

---

EXPLANATION OF PLATE 6

Figs 1–4. *Angulotreta postapicalis*. 1, F14902C; detail of an intralaminar, inwardly facing surface of a ventral valve showing the granular floor and the fabric of elongate domes, ×4800. 2, F14902A; detail of laminae in a fracture section of the apical region of a ventral valve showing a mesh-like infill between two lamellae penetrated by the holes of horizontally disposed canals, ×4800. 3–4, F14902A; details of columns in a fracture section through the apical region of a ventral valve; 3, a noded column, ×3500; 4, showing the degree of recrystallization of columns and the separation of lamellae in consecutive lamellae (in the bottom part of the figure), ×5200.

Figs 5–6. *Apsotreta expansa*. 5, F14903; detail of a partly recrystallized inner lamella (top right-hand corner) and of cross-sections through two columns showing the centripetal arrangement of acicular crystallites, ×7500. 6, detail of a cross-section through a partly recrystallized column surrounded by accretionary prisms of apatite, ×11300.

All scanning electron micrographs.

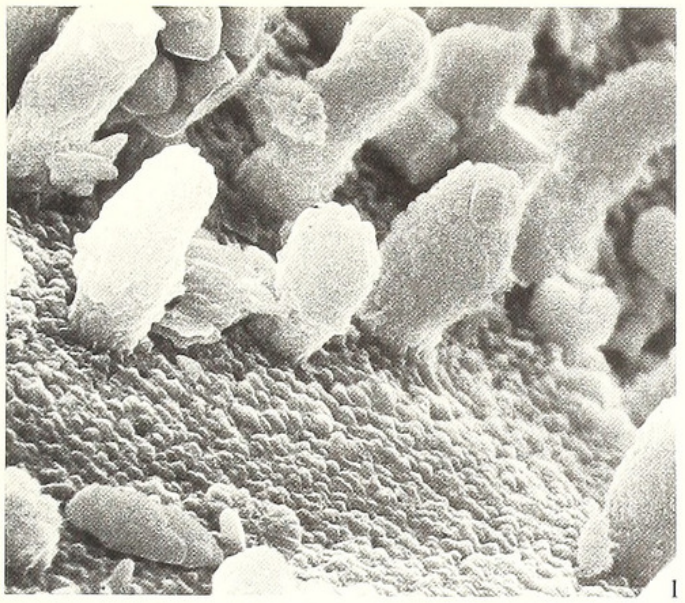
1

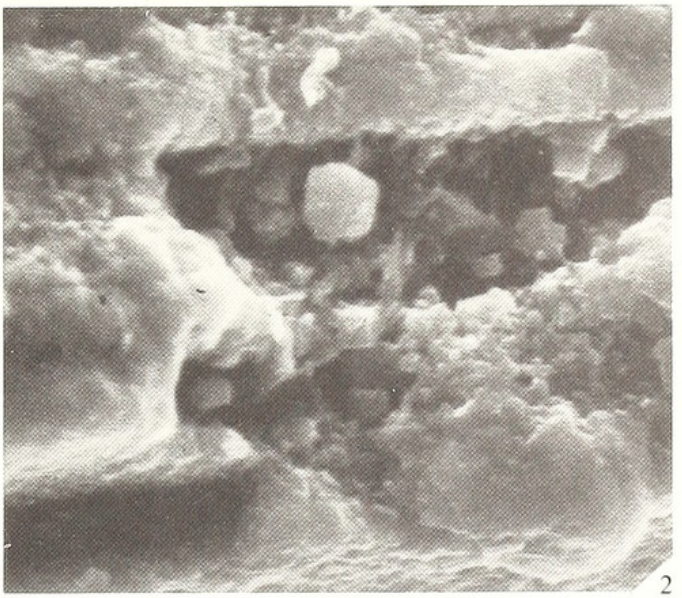
2

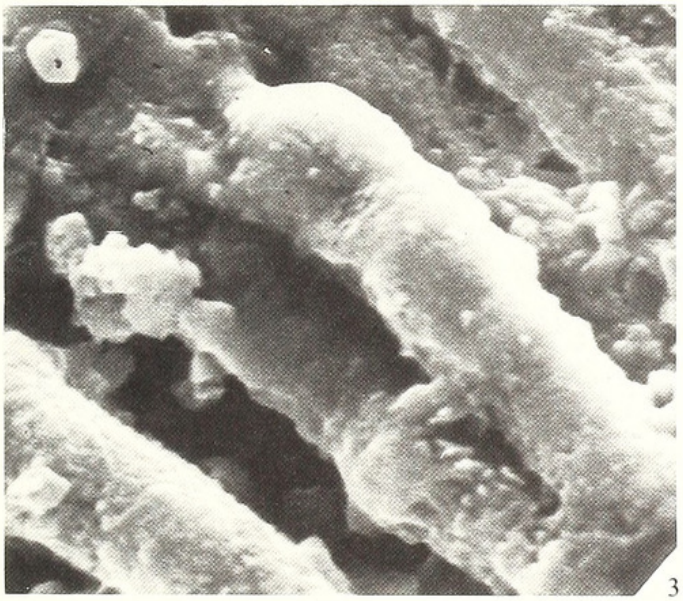
3

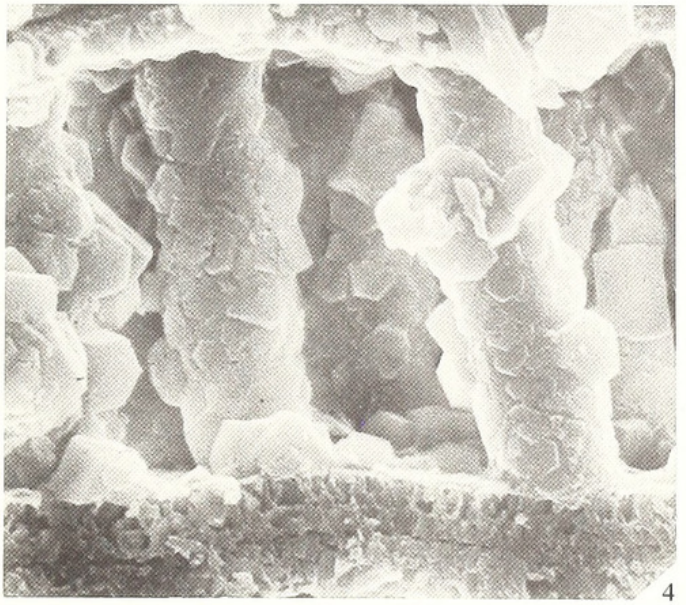
4

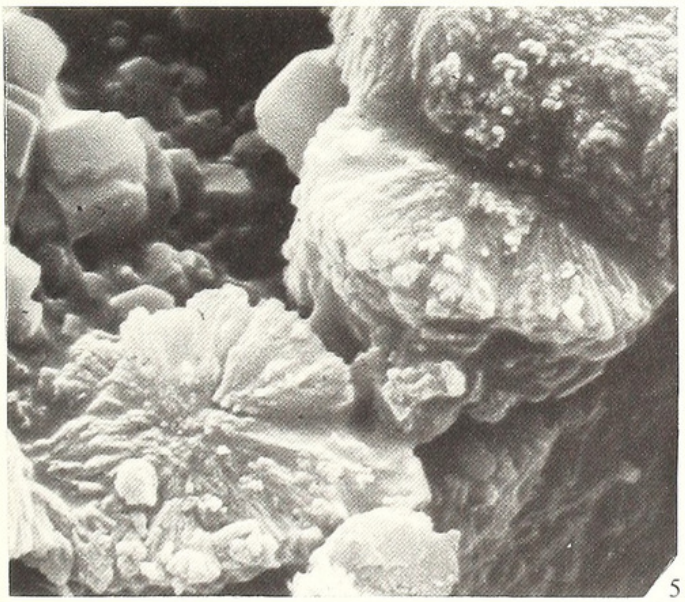
5

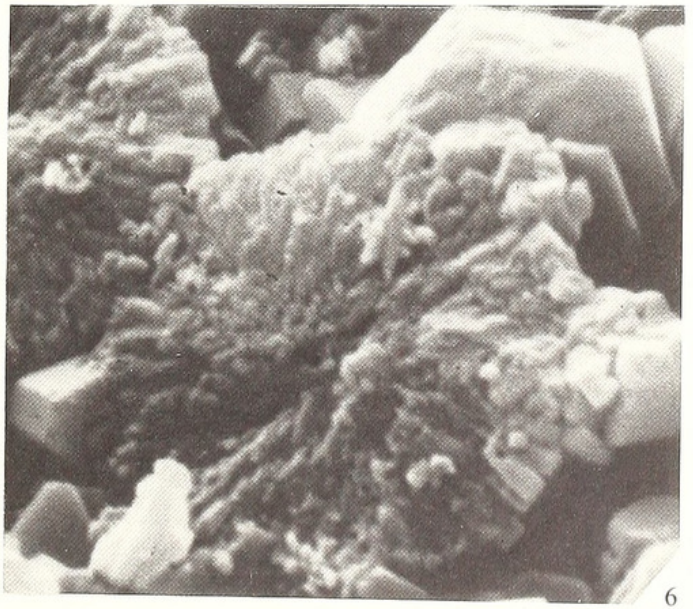
6

WILLIAMS and HOLMER, *Angulotreta*, *Apsotreta*

dried whole mounts of *Discinia striata* (Schumacher), is that the first-formed periostracum may be thrown into rounded concentric folds sporadically indented by radial grooves accommodating the outer surfaces of adpressed setae (Pl. 7, fig. 6).

The microstructures of the acrotretoid shell indicate that it, too, was secreted in the same way by an outer mantle lobe (Text-fig. 10). In effect, the external shell surface is the fossilized version of the apatite coat immediately underlying a periostracum which is no longer preserved; and its microstructures are moulds either of the periostracum as a whole or of the periostracal inner bounding membrane which itself could have acted as a moulding medium for the outer plasmalemmas of the secreting epithelium. Both such structures are found on the acrotretoid shell and the very fine scale of their preservation suggests that the first-formed biomineral coat was a cohesive paste of fine apatite crystallites suspended in an organic matrix comparable with mucopolysaccharide (Williams and Curry 1991, p. 138).

In this context, the networks of grooves, sporadically occurring on the exteriors of *Prototreta*, *Hisingerella*, etc., are casts of the outer plasmalemmas of epithelium just after they had secreted the inner sealing membrane of the periostracum. The grooves are casts of intercellular spaces bridged by tight junctions here and there. There are even casts of rare clusters of exocytosed, membrane-bound vesicles (Text-fig. 2; Pl. 2, fig. 1), some no more than 450 nm in diameter, which had evidently been incompletely incorporated into the sealing membrane of the periostracum before the secretion of the first coat of apatitic paste. However, the most revealing aspect of the casts is the striking similarity in the size and shape of the secreting plasmalemmas of the delineated epithelium with those of the vesicular cells in the outer mantle lobes of living brachiopods. The similarity is enhanced by the equally striking comparisons between the close-packed hexagonal network of grooves or ridges (Pl. 4, fig. 6) impressed on the internal surfaces of acrotretoids like *Linnarssonella* and *Cyrtonotreta* and those found on the valve floors of living inarticulates, in particular *Lingula* (Williams 1990, pl. 149E) and *Crania* (Williams and Wright 1970, p. 26). The last are known to be casts of cuboidal epithelium of the mantle, especially the patches underlying muscle bases. They add substance to our interpretation of hexagonally arranged partitions of the camerate partitions of *Cyrtonotreta* as having coincided with intercellular boundaries. The occurrence of both types of impressions on appropriate surfaces of the shells of acrotretoids confirms the epithelial differentiation in this extinct group was the same as that characterizing the differing secretory roles of the outer mantle lobe and mantle of living brachiopods.

EXPLANATION OF PLATE 7

Figs 1–2. *Hisingerella tenuis*. 1, Br 128496; general view of the posterolateral margin of the interior of a dorsal valve showing the partitions of the secondary camerate laminar layer being deposited at the time of death; the relatively featureless intramarginal floor represents an interlaminar surface, × 225. 2, Br 128496; oblique view of the margin of a dorsal valve showing the disposition of partitions in the various stages of completion relative to the outer lamella (bottom right-hand corner) and the inner lamella (top left-hand edge of micrograph), × 2550.

Fig. 3. *Scaphelasma mica*. Br 128547; general view of the posteromedian interior of a ventral valve showing the transition of radially disposed partitions into trails of dome-like bodies which become densely distributed posteriorly, × 280.

Fig. 4. *Hisingerella tenuis*. Br 128525; detail of fractured margin of a dorsal valve showing the intrapartition slots within partitions subtended between the outermost lamella of the secondary camerate layer (bottom part of micrograph) and the confining inner lamella, × 4200.

Fig. 5. *Glottidia pyramidata*. L14895; anteromedian view of the external surface of a dorsal valve showing sets of drapes deforming the periostracum, × 650.

Fig. 6. *Discina striata*. L14896; general view of inner mantle lobe of inner epithelium (lower right-hand corner) and the first-formed periostracum bearing grooves which accommodate setae arising from the inner mantle lobe, × 850.

All scanning electron micrographs.


1

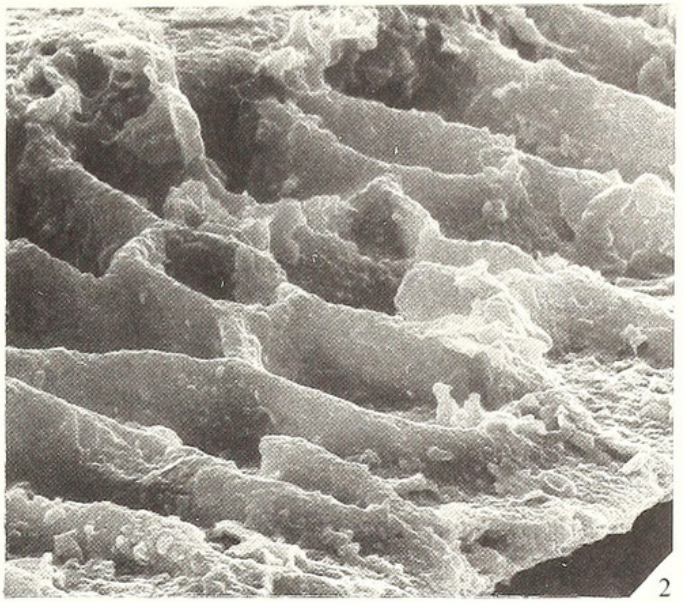
2

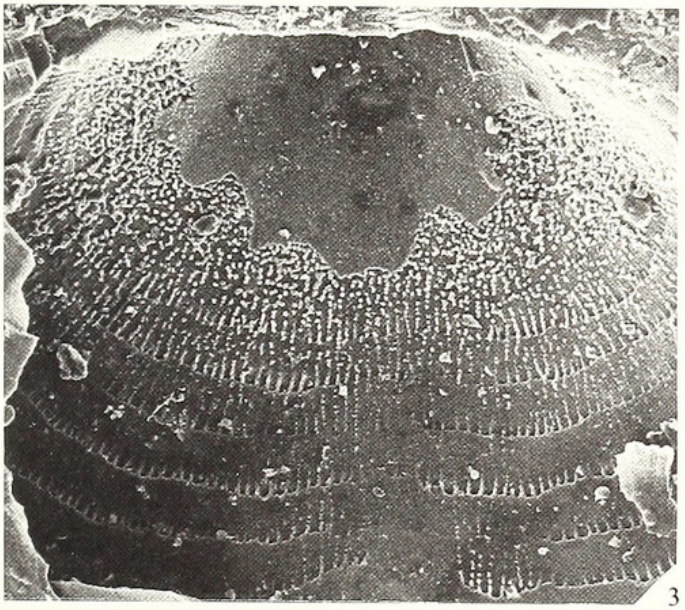
3

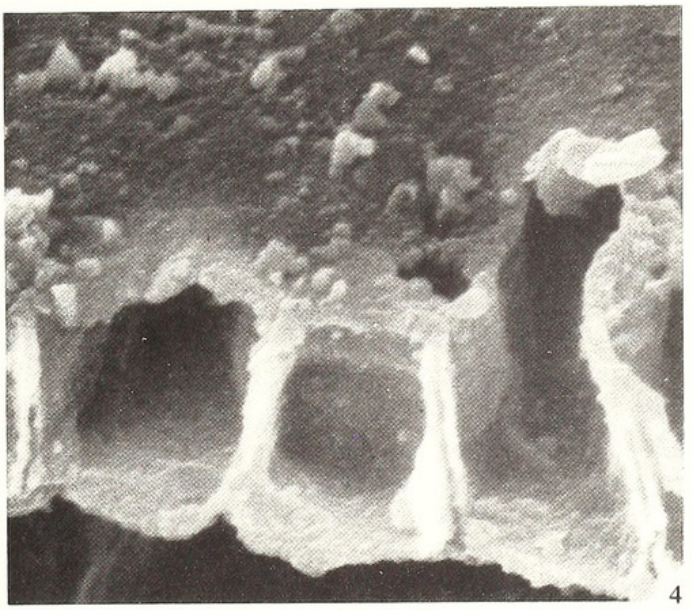
4

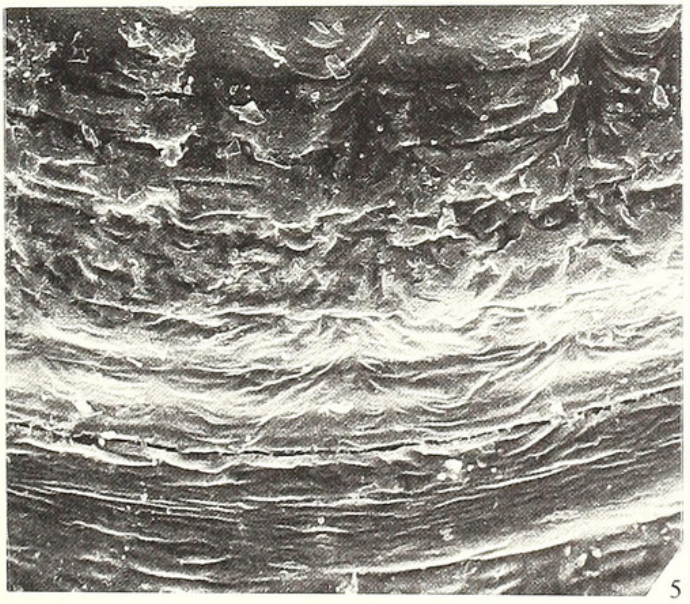
5

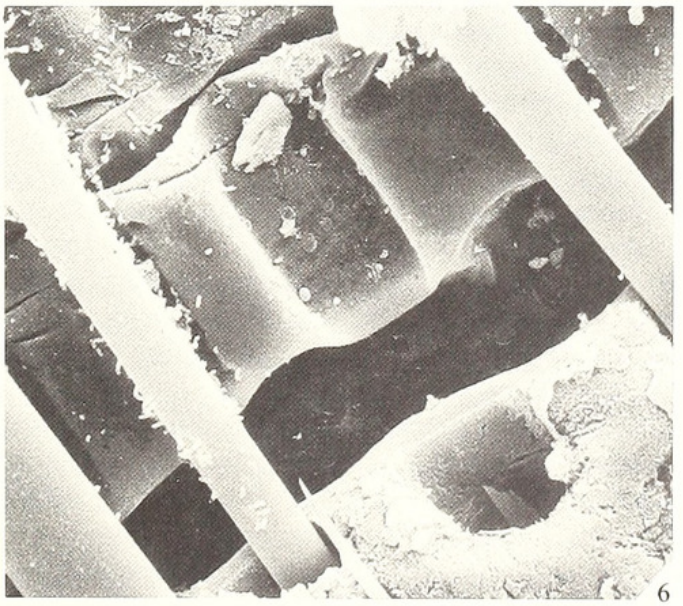
6

WILLIAMS and HOLMER, inarticulate brachiopods

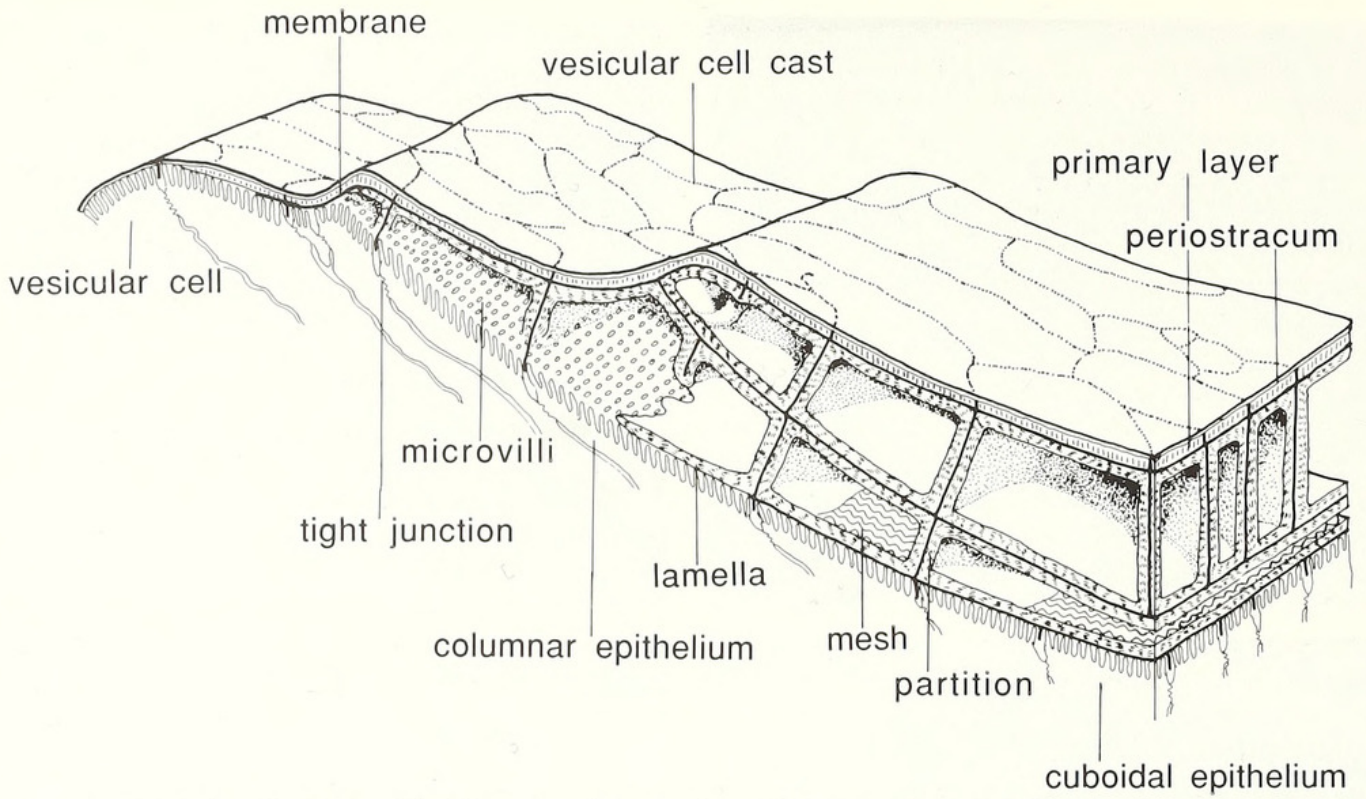

TEXT-FIG. 10. Inferred relationships between the mantle and its outer lobe and the valve margin of living *Hisingerella* (see also Pl. 7, fig. 1).

The ultrastructure of the acrotretoid periostracum has already been inferred from the nature of the pits indenting the larval shell, which have been interpreted as the moulds of exocytosed, membrane-bound vacuoles (Biernat and Williams 1970, p. 497). Since hemispherical pits may be 2 μm or more in diameter, the main part of the periostracal succession must have been somewhat thicker to accommodate such vesicles which would have been closely packed in an organic matrix (Text-fig. 1). This inferred periostracal succession is comparable with that of the articulate rhynchonellide *Notosaria*, which consists of a micron-thick, mucoproteinous layer with occluded vacuoles contained between a fibrillar, outer bounding unit membrane and an inner bounding unit membrane (Williams 1968, p. 271). The latter membrane is usually so thickened by additional proteinous exudation as to mask any microtopographical changes in the mucoproteinous layer resulting from the presence of vacuoles.

A thickened inner bounding membrane must also have been secreted by the vesicular cells of acrotretoids in the post-larval stages of shell growth. The sudden fading of the pit casts of flattened vesicles of *Linnarssonella* (Pl. 1, fig. 2) and *Opsiconidion* at the edge of the larval shell suggests that the onset of juvenile growth was heralded by an abnormal thickening of the periostracal inner bounding membrane rather than by a reduction in the exocytosis of vacuoles during the secretion of periostracum by the vesicular cells at the outer mantle lobe. This is borne out by the fact that, whereas imprints of the discoidal vesicles of *Linnarssonella* fade without dimunition of size, moulds of the spherical vesicles of *Angulotreta* become smaller as well as shallower towards the margin of the larval shell (Pl. 1, fig. 1).

Irrespective of the precise thickness and ultrastructure of the acrotretoid periostracum, it was evidently exuded as a flexible layer capable of registering wrinkles less than 1 μm in wavelength, such as those seen in living *Discina*. The outmost layer of the underlying shell must also initially have been flexible and certainly fine enough in texture to form moulds within the nanometric range before polymerizing as a biomineralized skin underlain by successive coats of apatite. In short, both layers, when subjected to stress, initially acted as ductile bodies which became increasingly brittle

after polymerization so that features of plastic deformation and brittle rupture have been recorded and may be used to reconstruct causal stress fields.

Thus, most shell damage seems to have arisen as fractures in the brittle shell, but was subsequently repaired by secretory activity in the plastic biomineral zone at the mantle edge. Here, stress couples would have been set up by differential growth rates within the area of damage and would have brought into being appropriately orientated folds and tension gashes (Text-fig. 4A). With further shell growth, the stress fields would have been subjected to radial rotation which would account for the eventual radial disposition of shell repairs regardless of the original orientation of fractures.

The fold systems imprinted on acrotretoid exteriors must have been caused by stresses affecting the plastic zone of the shell at the mantle edge. Indeed, the finer folding (F_1) which is superimposed on, and therefore deformed by, the coarser system (F_2), most likely originated as wrinkles of the periostracum immediately after the secretion of the inner sealing membrane slightly within the edge of the outer mantle lobe. Folds, running obliquely across fila as well as those splaying anteriorly from a point, were probably formed by radial couples induced by the differential growth of the periostracum itself.

The coarser (F_2) folding and segmentation of fila can also be interpreted in terms of stress fields with the maximum and intermediate principal stresses operating parallel with the interface between the periostracum and the underlying mineralized layer at the shell margin. The flat interspaces normally separating two adjacent sets of drapes advanced at a slower rate of shell accretion than the outwardly convex drapes themselves. These vectors of differential growth would have given rise to radial stress couples; and ancilliary features, including the streamlining of drapes and the culminations and depressions in their crest lines, are indicative of similar folding in a highly viscous medium. However, as already shown, some of the folding seems to have been literally skin-deep. Windows in the superficial mineralized coat, which reveal the fabric of the shell immediately below, show that the main fila are composed of evenly-bedded layers less than 500 nm thick, which were unaffected by ancilliary folding registered at the surface.

Anomalous as the F_2 of *Prototreta* may seem, it too could have been the result of radially directly stresses (Text-fig. 4C). The most novel features, the radial trails, are made up of antiforms such as would have been generated by maximum principal stresses acting anteroradially, while filar projections which face each other trace radial paths of principal compressive strain.

Acrotretoid biomineral succession

The mineral components of the exoskeleton of living brachiopods are intimately associated with the organic contents which can exceed 50 per cent of the dry weight of lingulids (Jope 1965, p. H157) and which are manifest as proteinaceous or chitinous sheets, membranes and strands as well as papillose outgrowths of the mantle, accommodated within permeating canals (punctae). These intraskeletal proteinaceous and chitinous constituents afford seeding surfaces for the biomineral components. The resultant interfaces are structurally distinguishable from surfaces of crystallization on a mineral substrate. The former are smooth, the latter roughened by crystalline microtopography. The contrast is well seen in the terminal faces of the secondary fibres of articulate brachiopods like *Notosaria* (Williams 1990, pl. 143B).

The relatively smooth textures of mineral surfaces seeded on organic substrates facilitate the reconstruction of fossil shell successions which have lost their organic framework. Thus, within the biomineral skeleton of acrotretoids, such surfaces bound the interlaminar and intrapartition slot-like gaps. They are also typical of the columnar canals (Holmer 1989, fig. 23D) which are known to connect with the slots between successive laminae. This distribution leads to the conclusion that the slots and the canals were originally occupied by sheets and strands respectively composed of proteins and/or chitin (Text-fig. 7).

The sheets, which would have filled slots less than 250 nm wide, could have been thickened unit membranes completely enveloping laminae in much the same way as those enclosing the secondary fibres of articulate brachiopods. They would, however, have differed in the mode of their secretion.

The interlaminar membranes would have been continuous with one another marginally to form a single sheet separating the edges of successive laminae from the overlying primary apatitic layer. But each interlaminar membrane would have been secreted separately and synchronously as a complete organic cover to the inner lamella of a fully developed lamina (see Pl. 7, fig. 1). It would then have served as the seeding sheet for crystallizing granules of apatite coalescing to form the interlaminar surface of the outer lamella of the succeeding lamina. In short, the basic organic framework of the acrotretoid skeleton consisted of a succession of subcircular, flattened envelopes, within which the apatitic and organic components of the shell were further segregated. The presence of intercalated laminae is consistent with this model as they represent localized acceleration of the same secretory cycle.

Accepting that organic sheets once filled the mid-slots of the intralaminar partitions, they would have been continuous with the interlaminar ones and could also have been thickened membranes. Moreover, there is evidence to suggest that the partitions coincide with impressions of cell boundaries. It is, therefore, reasonable to assume that the partition membranes were built up of compounds exuded through intercellular pathways (Text-fig. 7). As a result, a camerate lamina would have been subdivided into a single layer of membrane-covered boxes, each having the outline of an underlying cell which would have secreted into the box, as it took shape, the full range of the biomineral constituents of the acrotretoid shell. Bearing in mind the composition of the chitino-phosphatic shell of living species, the constituents are assumed to have been calcium and phosphate ions as well as their biogenic associates such as hydroxyproline, glycerine-rich proteins and chitin (Jope 1965, p. H161). Thus, a membranous box, continuously lined with appropriate bits of paired outer and inner lamellae and of the inwardly facing walls of four contiguous partitions, is identical to a fully developed lamina except in shape.

A question now arises as to whether the biomineral constituents of the membrane-bound compartments making up camerate laminae were still in solution or suspension when the compartments became sealed bags. It is more likely that precipitation and polymerization of the various constituents took place as the confining membranes were being secreted. The nucleation of biominerals concomitantly with the growth of seeding sheets is the common mode of shell secretion in living brachiopods. The shell fabric of living chitinophosphatic lingulids and discinids also shows how apatite, proteins and chitin can occur together in an unstratified fashion in intralaminar spaces. The apatite may occur as interconnected or isolated rods, lenses or incomplete granular jig-saws in an anastomosing organic 'mesh' (Text-fig. 10). Chemical removal of the organic components, in simulation of fossilization, leaves mineral configurations comparable, at least morphologically, with those found in acrotretoid shells (compare Pl. 6, fig. 2).

According to this interpretation, the secretory cycle giving rise to a camerate unit of a lamina would have proceeded with: (1) the nucleation of apatite granules to form a thickening layer on the inner face of an interlaminar membrane and on the inward-facing, intrapartition membranes as they grew; (2) the simultaneous secretion of an interwoven mesh of apatite with crystallites and polymer configurations within the space contained by the thickening apatitic layer; and (3) the sealing of the unit by the deposition of another interlaminar membrane with granular apatite nucleating on its outer and inner surfaces.

The growth of intralaminar columns and domes could have proceeded in the same way as the secretion of partitions, but with apatite coating variable lengths of organic strands instead of sheet-like membranes to account for the axial canals of the columns. It is presently not possible to determine whether the canals were filled with extensions of outer epithelium like those permeating chitinophosphatic shells of living species. However, the diameters of acrotretoid canals, which vary widely from about 500 to over 900 nm, are comparable with those of living *Discina* (300–600 nm) and *Discinisca* (350–850 nm). On balance, we assume that acrotretoid canals were lined with a unit membrane which enclosed vesicles, some with mucoproteins as have been found in *Lingula* (Williams and Mackay 1979, p. 726). The canal diameters are also much the same as the pits and depressions found on interlaminar surfaces (see Pl. 4, fig. 5) indicating that the epithelial extensions would have been continuous with the putative interlaminar membranes. Indeed, it is assumed that

such epithelial extensions would have breached interlaminar membranes wherever columns are continuous from one lamina to the next.

Domes are more difficult to interpret despite their micromorphological similarity to columns. No canal has yet been seen penetrating the free, rounded end of a dome although slight depressions can occur (see Pl. 5, fig. 5). It therefore seems more likely that domes were seeded, in spherulitic arrays, on solid, impersistent attachments to the inner surfaces of interlaminar membranes, like hemidesmosomes. It has to be conceded, however, that some cylindroid outgrowths with axial canals, which had been fractured near their bases, may have been broken domes not columns. Indeed, the difference between the organic core of a dome and that of a column could have been merely their lengths rather than their composition.

Any attempt to establish the original structure and composition of the acrotretoid shell has constantly to distinguish between the products of biomineralization and post-mortem recrystallization. The distinction is critical as the presence of intralaminar spaces within acrotretoid shells prompts questions as to whether they were empty *in vivo* or filled with biogenic materials which were subsequently lost, redistributed or replaced during fossilization. As indicated above, the development of domes, columns and partitions favours the presence of biogenic materials within the intralaminar spaces in living acrotretoids. We further believe that the apatitic component of the infill can exceptionally survive *in situ* as a granular mesh (see Pl. 6, fig. 2) from which all organic interweaves have been removed by hydrolysis. More frequently, the biomineral infill underwent *in situ* recrystallization to form the cryptocrystalline calcium phosphate (CCP). It could also have been dissolved during diagenesis and transported elsewhere to leave empty camerae or recrystallized, as secondary accretions of pinacoidal plates, prisms and so on, on the original apatitic coats forming the lamellae, partitions, domes and columns (see Pl. 6, figs 5–6). The original coats are also likely to have undergone recrystallization; but they usually become more compact and are distinguishable from the more open crystalline fabric of the post-mortem deposits.

Our conclusions on the nature of the shell of living acrotretoids are at variance with all those reached in previous researches, although we shall limit our review of other interpretations to those aided by the electron microscope.

Poulsen (1971) first reported the existence of camerate and columnar laminae in an unnamed Ordovician species, now believed to be an acrotretine (Holmer 1989, p. 49). Poulsen concluded (1971, pp. 268–269): that empty intralaminar spaces had originally contained organic material; that the columns were phosphatic moulds of cytoplasmic strands (although he did not rule out a primary origin); and that the partitions of the 'outer' camerate layer were secreted 'along the entire free periphery of larger cells' which alternated at the mantle edge with 'smaller' cells exuding interpartition organic material. It should be noted at this juncture that Holmer (1989, p. 49) accepted the empty intralaminar spaces as having contained an organic matrix but queried the phosphatization of the punctae.

The original state of the acrotretoid shell has also been considered by Rowell and Henderson (1978, p. 4) and by Rowell (1986, p. 1062). They were undecided as to whether intralaminar spaces had contained organic material or had been empty in the living state, an alternative which is hardly tenable.

However, the most far-reaching studies of the acrotretoid shell structure have been carried out by Ushatinskaya *et al.* (1988, p. 54). Thus, the 'outer layer' of the Upper Cambrian *Treptotreta*, which seems to have comprised the wedge-shaped margins of successive camerate laminae, is described as a phosphatized periostracum resembling that of *Discinisca* (Williams and Mackay 1979, p. 730). Any such resemblance, as they admit, arises from the poor preservation of the distal edges of the outer lamellae; and in every other respect does not bear scrutiny. The columns and their confining lamellae are also interpreted as being phosphatized canals and organic layers of the shell, respectively. Even the partitions of the camerate shell (Ushatinskaya 1990, p. 58) are interpreted as phosphatized organic structures. This postulated wholesale mineralization of the acrotretoid organic framework is ascribed to the 'diagenetic redistribution' of the calcium phosphate of the biomineral layers within the living shell (Ushatinskaya *et al.* 1988, p. 47). In this context, the 'double

lamina' of Ushatinskaya *et al.* is equivalent to adjacent outer and inner lamellae of two adjacent laminae in our model (Text-fig. 7). It is regarded by them as confirmation that a single organic layer had been diagenetically phosphatized from above and below.

This interpretation of the biomineralization of the acrotretoid shell is diametrically opposed to the one given here. In that respect, the evidence against the assumptions of Ushatinskaya and her colleagues has already been presented. It led us to conclude that the original organic framework of the acrotretoid shell is not represented by the phosphatic structures of its fossilized remains, but by slots, canals and spaces therein.

NATURE OF THE ACROTRETOID MANTLE

In living brachiopods, the outer epithelium of the mantle and its marginal lobe is differentiated into three basic types: lobate cells, occupying a narrow band on the inner side of the outer mantle lobe between the periostracal slot and the mantle groove; vesicular cells, forming most of the lobe; and cuboidal cells, characterizing the main spread of the mantle. A similar differentiation of the acrotretoid mantle can also be inferred except for the existence of the lobate cells (Text-fig. 10). These are responsible for secreting the periostracal superstructure, like the multilaminar concentric ridges of discinids (Williams and Mackay 1979, p. 734), which features are presently unknown in the fossil state and, in any event, are not germane to our understanding of the acrotretoid secretory regime. Accordingly, no special feature has been attributed to the acrotretoid lobate cells. The main problem is to distinguish the respective roles of the vesicular and cuboidal (and columnar) epithelium in the secretion of the inferred periostracum, the identifiable primary layer and the underlying secondary and tertiary successions of camerate and columnar laminae.

As already indicated, the thick vesicular basal layer of the periostracum and the finely textured organo-mineral primary layer are assumed to have been flexible sheets although only the latter is preserved in the fossilized state. The periostracum would certainly have been secreted by the vesicular cells on the inner face of the outer mantle lobe with the outer bounding membrane exuded within the periostracal slot and the vesicular layer and its sealing, inner bounding membrane secreted by the more distal part of the lobe. The succeeding primary layer must also have been secreted by vesicular cells as well as the underlying edges of laminae in order to account for the way camerate partitions trace the characteristic outlines of these cells. Since the laminar edges are inflexible components of the shell, they must have been secreted by the vesicular cells at the outer surface of the outer mantle lobe (Text-fig. 10).

The radial length of the acrotretoid mantle lobe may be deduced from the structure of the internal margin of a dorsal valve of *Hisingerella tenuis* Holmer (Pl. 7, figs 1–2). As one would expect, the lamina, being secreted at the moment of death, forms the floor of the valve. It consists of the interlaminar surface of the inner lamella which, however, is absent marginally to reveal the partitions which were being secreted in the wedge-shaped fringe of the lamina. This partitioned margin would have coincided with the outer surface of the outer mantle lobe which must have been at least 22 μm long compared with the valve's sagittal length of almost 0·5 mm. It is noteworthy that there is no trace of a primary layer peripheral to the partitioned fringe of this specimen. Such absence confirms the fragility of the primary layer which, nothwithstanding, must have been continuously deposited beyond the expanding edge of the laminar shell. There is, however, no indication as to whether this marginal fringe of primary apatite was deposited in the plane of the secondary shell by the outer surface of the lobe, or whether it was introverted and secreted by the inner surface of the lobe as in lingulids. We have figured the layer as having been deposited on the outer surface of the outer mantle lobe.

The dynamics of shell secretion are not easily portrayed. However, sections like those of the columnar laminae of *Myotreta dalecarlica* (see Holmer 1989, fig. 31) can be stylized as consecutive views of the radial expansion of laminar margins relative to the secreting epithelium. In Text-figure 11, a hypothetical section of a valve with secondary camerate laminae has been re-cast to show how successive wedge-shaped laminar margins could have been secreted by an advancing outer mantle

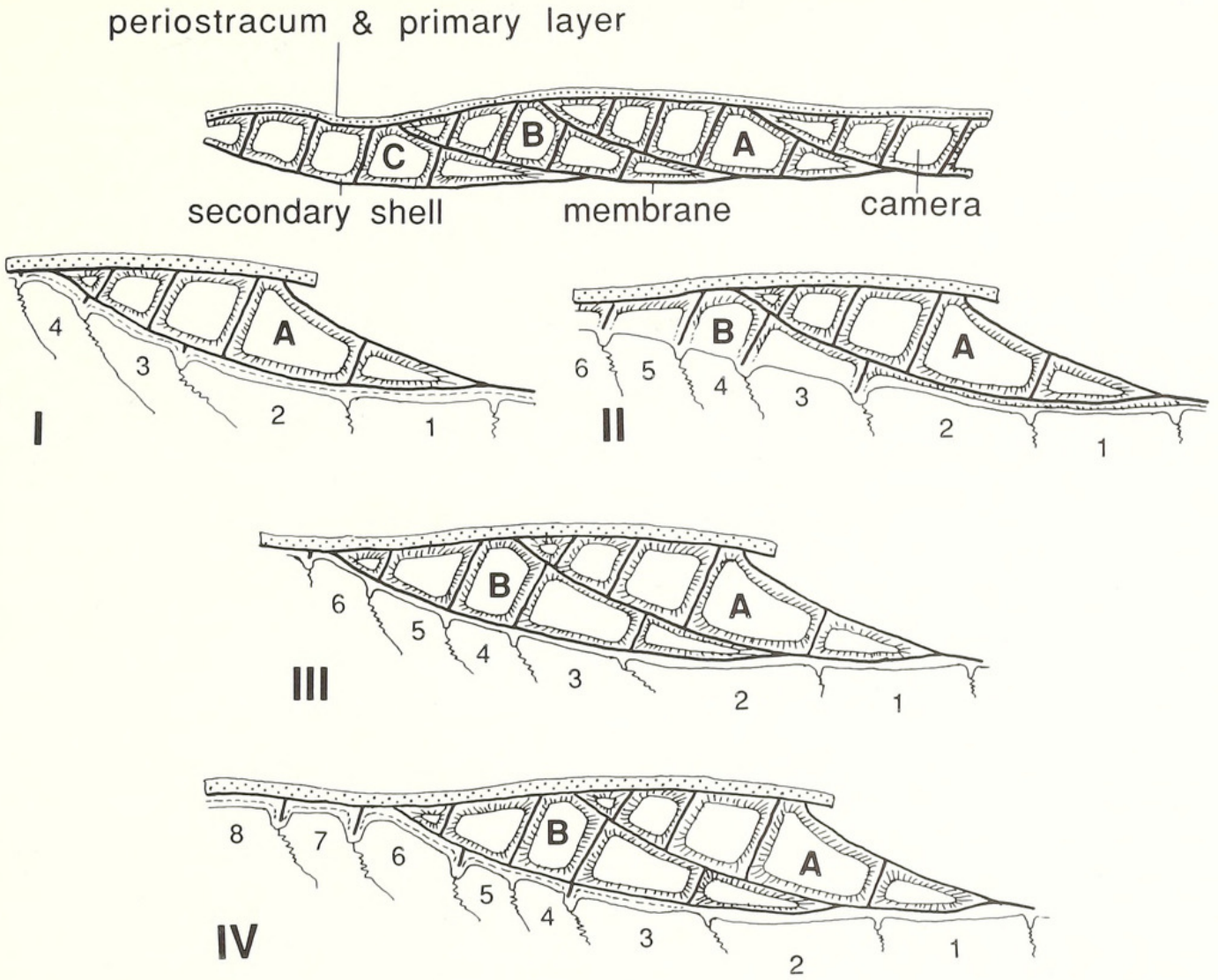

TEXT-FIG. 11. Stylized representation of the inferred growth of two camerate laminae (A and B) accompanied by the anteroradial generation of secreting shells (5–8) as seen in four successive stages (I–IV) of marginal expansion of an acrotretoid valve.

lobe which expanded by the addition of new vesicular cells at its tip. Text-figure 11 also shows how cuboidal epithelium (represented by cell 1 in the diagram) could have sealed off an entire lamina (A) with an interlaminar membrane which then became a seeding sheet for the succeeding lamina (B). The transgression of the tapering proximal part of lamina B across the wedge-shaped, distal margin of lamina A is not a junction between secondary and tertiary layers, sharp as it may be. As already noted, the tertiary layer is structurally different from the rest of the shell. It is, of course, more easily identifiable when it is columnar in contrast to a secondary camerate layer as in *Conotreta*? *mica* Gorysanskji (Holmer 1989, fig. 23). In any event, it formed a distinct layer with a recognizable margin of its own; and would have been deposited by epithelium with a changed secretory regime. In the case of *C.*? *mica*, the change would have switched the deposition of apatite from intercellular pathways to many loci on the plasmalemmas of the secreting epithelium.

Finally, by attempting to explain the origin of the F_2 folds affecting the filar ornamentation of acrotretoids, one more assumption can be made about the mantle edge. In all living brachiopods, apart from cemented post-larval forms like *Neocrania*, the groove between the outer and inner mantle lobes is invaginated into a series of follicles bearing setae. The muscles serving the setal

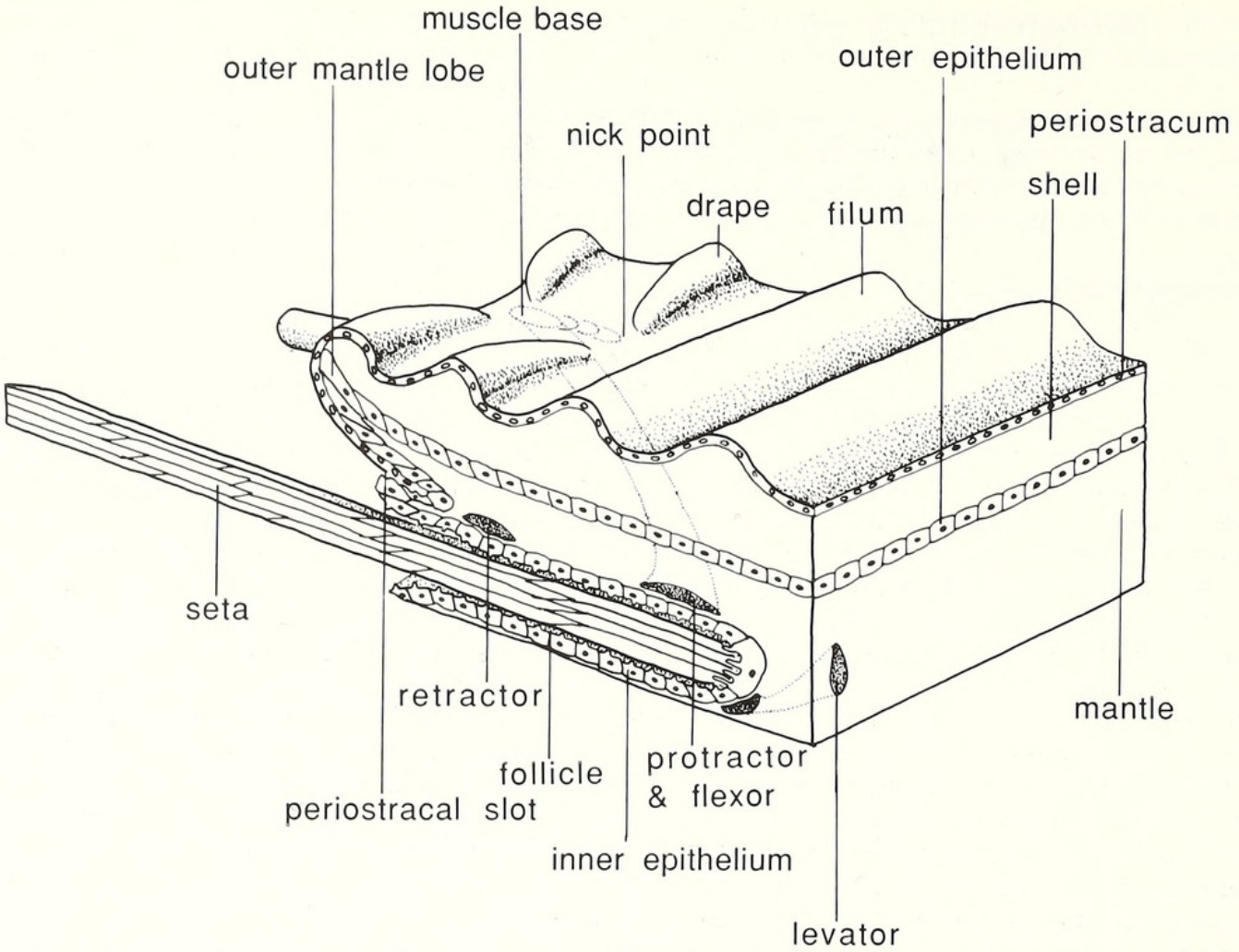

TEXT-FIG. 12. Inferred structure of the outer mantle lobe of living acrotretoids in relation to the shell, a follicle and the muscles controlling the seta, which are assumed to have been arranged as those found in living *Lingula*.

follicles are well-known only in *Lingula*. They include three diagonally operating sets (see Text-fig. 12): protractors and flexors attached to the inner ends of the follicles and to loci within the crests of the periostracal/outer epithelial fold at the shell edge; and retractors connecting the mantle with the periostracal groove (and the outer end of the follicle).

In attempting to attribute the F_2 folds of fila to functional aberrations in the growth of the acrotretoid shell, several criteria have to be satisfied. They include: (1) the essential symmetry of the folds about radial axes; (2) the impersistence of the folds along any one radial axis although they may recur several times along the same axis to the edge of the shell; and (3) the sporadic distribution of the folds over the shell surface except at interruptions of growth, in association with which they may become manifest as more or less continuous, concentric bands of drapes.

The symmetry of the folding is such that the interspaces between the converging ends of pairs of drapes (nick points) trace paths of restraining stresses relative to a forwardly directed force along the axial traces of the drapes themselves. The fact that the drapes seldom persist for more than 60 μm radially but may occur anywhere on the shell surface, suggests that they were generated by temporary abnormalities in growth which could affect any part of the mantle edge. Yet, when the drapes occur in concentric bands, they tend to have fairly constant chord lengths. The F_2 fold systems could, therefore, have been induced by the spasmodic activity of regularly occurring features of the mantle edge. The most obvious sources of such stresses would have been the muscle sets controlling the setal follicles in the mantle groove (Text-fig. 12).

The disposition of the protractors and flexors is especially relevant to this notion as their bases trace radially disposed intersetal zones of potential stress. Moreover, since bands of drapes are most commonly associated with growth lines, it seems reasonable to assume that the nick points of acrotretoid drapes represent the sites of muscle fibres that were under sufficient temporary stress to reduce the forward growth of the shell relative to expanding drapes overarching setae. In this context it is noteworthy that each of two otherwise smooth dorsal valves of *Glottidia pyramidata*, which were fixed in formalin some weeks after their despatch from Florida, bears a band of drapes (Pl. 7, fig. 5) associated with a break in the forward growth of the shell within 1 mm of the umbo. Measurements of 31 and 47 chords of drapes gave averages of 16·3 μm (range 5·5–21·8 μm) and 15 μm (range 7·4–32·4 μm), respectively. Such structures could have accommodated setae, which in a mature dorsal valve of *Glottidia* varied in width from 3·5 μm to 9·5 μm and had an average spacing of 29 μm (with a range from 14 μm to 58 μm) between the midpoints of 41 follicles. These estimates are consistent with the interpretation of the acrotretoid drapes as having overlain setal follicles and the nick points in the interspaces as having been the sites of follicular muscle systems. It is worth noting that concentric folds of the first-formed periostracum of *Discina* may also survive as impersistent arcs on the external surfaces of valves, although no radial grooves representing setal imprints have yet been found on them. Presumably, such imprints are normally erased by the elastic recovery of the periostracum as it is conveyed away from the proximal pressure exerted by the setal bases.

The use of drapes to determine the frequency of setae at various stages in the growth of the acrotretoid shell rests on two further assumptions. First, any increase in the number of post-larval setae has probably always been preceded by the division of the microvillous cell at the base of the follicle, which simultaneously becomes partitioned to house an ancillary seta being secreted by the new cell. This follicular budding can greatly affect the microarchitecture of the shell. In *Terebratulina*, for example, each rib normally accommodates a single seta with its follicle. But budding takes place before a subsidiary rib is separated from an earlier formed one by the intercalation of a concave interspace. As a result, a rib may temporarily house an ancillary seta as well as a mature one. This sequence of development could also have occurred beneath drapes and would account for the occasional arrangement of a broad drape succeeded anteroradially by two unequally narrow ones. The second assumption is that once follicles have been formed, they persist throughout life, each advancing radially along a unique path although the contained seta(e) may have been periodically shed. The fewest setae fringing an acrotretoid valve would, therefore, have been equal to the sum of all drapes excluding those that fall on the same radial trajectories of earlier formed nick points.

The reconstructions, some of which are given in Text-figure 13, reveal consistency of inferred setal frequencies among specimens of the same genus but variation between genera. In two dorsal valves of *Angulotreta*, at least 10 setae could have existed at the end of the larval stage of development and 34 and 43 at post-larval growth stages. A comparable range was found in two dorsal valves of 'acrotretoid A' when allowance is made for the larger larval shell of this genus. Nick points of 9 and 7 possible setae were found at the edges of the 0·3 mm wide larval shell, increasing to about 30 in post-larval stages when the valves were 0·5 mm wide. In contrast, 20 setae (including 2 extrapolated posteromedianly to fill obvious gaps) could have been present at the larval growth stage and 51 at the margin of a ventral valve of *Prototreta*; while only 17 nick points were found on a dorsal valve of acrotretoid B with a maximum width of 0·5 mm. Whether such variation is taxonomically important has yet to be tested; but a preliminary survey of relevant literature at least suggests that the occurrence of nick points is a widespread feature of acrotretoids and that adequate samples can be obtained to explore further their significance.

CONCLUSIONS ON THE AFFINITIES OF ACROTRETOID SHELLS

The wealth of microscopic features preserved on the exoskeletal surfaces of chitinophosphatic brachiopods is proving to be a source of valuable information about the mantle anatomy of fossil groups. The flexibility of chitinophosphatic shells has been known since living species were first

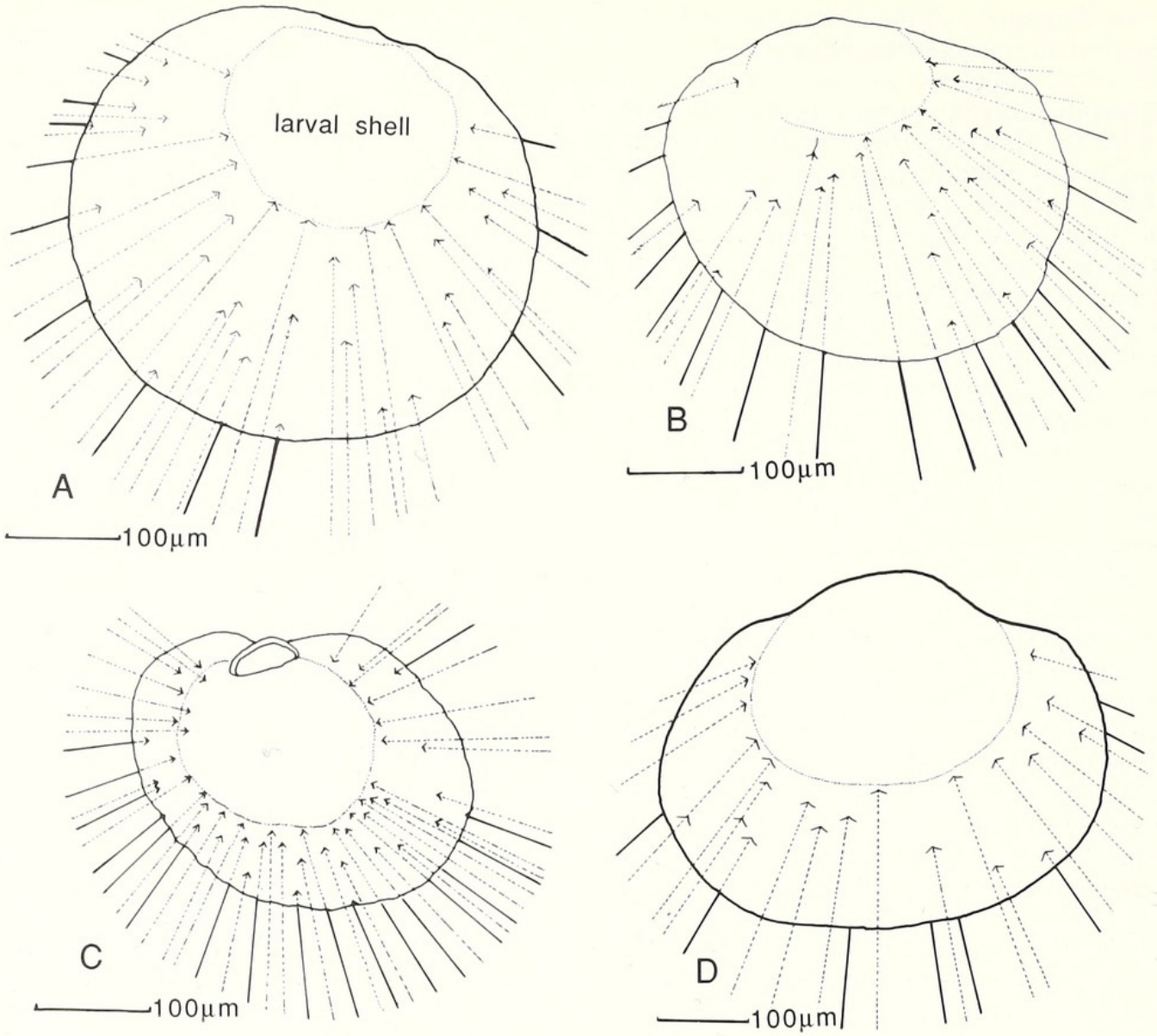

TEXT-FIG. 13. Inferred arrangement of setae in young dorsal valves of *Angulotreta* (A–B) *Prototreta* sp. (C) and 'acrotretoid A' (D); with the solid lines representing setae corresponding to nick points at the edge of a valve and dotted lines corresponding to intramarginal nick points which first became evident at the sites of the wide-angled Vs.

described. Yet only recently (Williams and Curry 1991) has it been noted that stress fields resulting from shell flexibility can induce plastic deformation of the exoskeleton, evidence of which survives as strain phenomena in the fossil state. Such flexibility reflects the composition of the chitinophosphatic shell, not just the comparatively high organic content but also the very fine crystalline form of its biomineral constituent. Inarticulate shell chemistry is still under active investigation in many institutions. But the emerging consensus of opinion (e.g. Watabe 1990, pp. 41–42) is that the prevalent biomineral unit of the living shell is an acicular crystallite, akin to francolite in composition and 30–40 nm thick and up to four or five times as long. The crystallites may be aligned with sheets of protein fibres, 5 nm in diameter, or aggregated into spherulites within a glycosaminoglycan network with strands also about 5 nm thick.

After secretion, the constituents of the chitinophosphatic shell will, therefore, polymerize into laminae (including clusters of amalgamated spherulites) which are texturally fine enough to register

distortions as well as casts of features larger than 30–40 nm. Recrystallization could, of course, destroy all traces of the original fabric but, judging from our experience so far, the prospects of these very fine structures surviving on the oldest of fossils are good. They are certainly more likely to be found on chitinophosphatic than carbonate shells. The crystalline units of calcitic or aragonitic shells are almost invariably too coarsely aggregated in too small a quantity of organic matrix to undergo small-scale plastic deformation. They may, however, form casts showing interruptions between discrete centres of crystal growth and, thereby, delineate structures measurable in microns, especially secretory plasmalemmas outlined by intercellular boundaries.

In our acrotretoid studies, the smallest original features found on shell surfaces were grooves interpreted as intercellular spaces about 100 nm across, associated casts of vesicles 450 nm in diameter (Text-fig. 2) and F_1 folds (Pl. 3, fig. 5) about 500 nm in wavelength. The scale of these structures is well within the limits imposed by the dominant fabric of granules, about 100 nm across. We have assumed this to be a primary fabric which is different from those composed of acicular crystallites and, therefore, possibly indicative of a different chitino-proteinaceous matrix. Further work on the biomineral ultrastructure of living as well as fossil species would test the validity of this apparent difference in texture.

The survival of casts of cell outlines on the shells of extinct brachiopods confirms what has already been shown for living species (Williams 1977, p. 117). So far as biomineral secretion is concerned, a morphological as well as a physiological distinction can be drawn between the flat-lying, elongate vesicular cells, responsible for secreting the periostracal base and the primary layer, and the cuboidal epithelium of the intramarginal mantle, which secretes the rest of the shell. As has been shown, this differentiation of the mantle was also characteristic of early Palaeozoic acrotretoids. In fact, it is unique to the Brachiopoda as presently understood by the great majority of students of the phylum. In molluscan bivalves, for example, the mantle edge is folded into three or four lobes and tall, columnar epithelium secretes the first-formed part of the biomineral succession (Watabe 1984, p. 465). Accordingly, this invariable differentiation of the outer mantle into the same types of epithelia refutes the views that the brachiopods were polyphyletic (Valentine 1975; Wright 1979; Goryanskij and Popov 1986). More intriguingly, the epithelial differentiation of the brachiopod mantle must have preceded the biochemical differentiation of the phosphatic and carbonate secretory regimes and suggests a close phylogenetic relationship between the resulting skeletal successions. In unravelling this relationship, the distinctiveness of the acrotretoid skeleton serves as a measure of the variation inherent in the secretory activities of the brachiopod mantle.

Acknowledgements. This work was undertaken when one of us (A.W.) held a research grant from the Royal Society and the other (L.E.H.) a grant from the Swedish Natural Science Research Council. We are indebted to both bodies for their support.

REFERENCES

BELL, W. C. 1941. Cambrian Brachiopoda from Montana. *Journal of Paleontology*, **15**, 193–255.

—— and ELLINWOOD, H. L. 1962. Upper Franconian and Lower Trempealeauan Cambrian trilobites and brachiopods, Wilberns Formation, central Texas. *Journal of Paleontology*, **36**, 385–423.

BIERNAT, G. and WILLIAMS, A. 1970. Ultrastructure of the protegulum of some acrotretide brachiopods. *Palaeontology*, **13**, 491–502.

BLOCHMANN, F. 1990. *Untersuchungen über den Bau der Brachiopoden 1. Die Anatomie von* Discinisca lamellosa *(Broderip) und* Lingula anatina *Bruguiere*. Gustav Fischer, Jena, 66–124 pp.

GORYANSKIJ, V. YU. and POPOV, L. E. 1986. On the origin and systematic position of the calcareous-shelled inarticulate brachiopods. *Lethaia*, **19**, 233–240.

HOLMER, L. E. 1989. Middle Ordovician phosphatic inarticulate brachiopods from Västergötland and Dalarna, Sweden. *Fossils and Strata*, **26**, 1–172.

JOPE, H. M. 1965. Composition of brachiopod shell. H156–H164. *In* MOORE, R. C. (ed.). *Treatise on invertebrate paleontology. Part H. Brachiopoda*. Geological Society of America and University of Kansas Press, Boulder, Colorado and Lawrence, Kansas, 927 pp.

PALMER, A. R. 1954. The faunas of the Riley Formation in central Texas. *Journal of Paleontology*, **28**, 709–786.

POPOV, L. E. and USHATINSKAYA, G. T. 1986. O vtorichnykh izmeneniyakh mikrostructury fosfatno-kal'tsievykh rakovin bezzamkovykh brakhiopod. [On secondary changes in the microstructure of calcium-phosphatic shells of inarticulate brachiopods.] *Izvestiya Akademii Nauk SSSR, Seriya Geologicheskaya*, **10**, 135–137. [In Russian].

POULSEN, V. 1971. Notes on an Ordovician acrotretacean brachiopod from the Oslo region. *Bulletin of the Geological Society of Denmark*, **20**, 265–278.

ROWELL, A. J. 1986. The distribution and inferred larval dispersion of *Rhondellina dorei*: a new Cambrian brachiopod (Acrotretida). *Journal of Paleontology*, **60**, 1056–1065.

—— and HENDERSON, R. A. 1978. New genera of acrotretids from the Cambrian of Australia and the United States. *The University of Kansas Palaeontological Contributions*, **93**, 1–12.

USHATINSKAYA, G. T. 1990. Microstruktura i sekretsiya rakoviny y bezzamkovykh brakhiopod otryada Acrotretida. [Microstructure and shell secretion in inarticulate brachiopods of the Order Acrotretida.] *Paleontologicheskij Zhurnal*, **3**, 55–65. [In Russian].

—— ZEZINA, O N., POPOV, L. YE. and PUTIVTSEVA, N. V. 1988. O mikrostrukture i mineral 'nom sostave brakhiopod of fosfatno-kai'tsiyevoy rakovinoy. [On the microstructure and composition of brachiopods with calcium phosphate shell.] *Paleontologicheskij Zhurnal*, **1**, 45–55. [In Russian].

VALENTINE, J. W. 1975. Adaptive strategy and the origin of grades and groundplans. *American Zoologist*, **15**, 391–404.

WATABE, N. 1984. Mollusca: Shell. 449–485. *In* BEREITER-HAHN, J., MATOLTSY, A. G. and RICHARDS, K. S. (eds). *Biology of the integument. 1 Invertebrates*. Springer-Verlag, Berlin, 841 pp.

—— 1990. Calcium phosphate structures in invertebrates and protozoans. 35–44. *In* CARTER, J. G. (ed.). *Skeletal biomineralization: patterns, processes and evolutionary trends. Volume I.* Van Nostrand Reinhold, New York, 832 pp.

WILLIAMS, A. 1968. A history of skeletal secretion among articulate brachiopods. *Lethaia*, **1**, 268–287.

—— 1977. Differentiation and growth of the brachiopod mantle. *American Zoologist*, **17**, 107–120.

—— 1990. Biomineralization in the lophophorates. 67–82. *In* CARTER, J. G. (ed.). *Skeletal biomineralization: patterns, processes and evolutionary trends. Volume I.* Van Nostrand Reinhold, New York, 832 pp.

—— and CURRY, G. B. 1991. The microarchitecture of some acrotretide brachiopods. 133–140. *In* MACKINNON, D. I., LEE, D. E. and CAMPBELL, J. D. (eds). *Brachiopods through time*. A. A. Balkema, Rotterdam, 447 pp.

—— and MACKAY, S. 1979. Differentiation of the brachiopod periostracum. *Palaeontology*, **22**, 721–736.

—— and ROWELL, A. J. 1965. Morphology. H57–H155. *In* MOORE, R. C. (ed.). *Treatise on invertebrate paleontology. Part H. Brachiopoda*. Geological Society of America and University of Kansas Press, Boulder, Colorado and Lawrence, Kansas, 927 pp.

—— and WRIGHT, A. D. 1970. Shell structure of the Craniacea and other calcareous inarticulate brachiopods. *Special Papers in Palaeontology*, **7**, 1–51.

WRIGHT, A. D. 1979. Brachiopod radiation. 235–252. *In* HOUSE, M. R. (ed.). *The origin of major invertebrate groups*. Academic Press, London, 515 pp.

ALWYN WILLIAMS
Palaeobiology Unit
Department of Geology and Applied Geology
University of Glasgow
8 Lilybank Gardens, Glasgow G12 8QQ, UK

LARS E. HOLMER
Paleontologiska institutionen
Uppsala Universitet
Box 558, S-751 22 Uppsala
Sweden

Typescript received 1 May 1991
Revised typescript received 28 June 1991